LA-13098

Verification of the Monte Carlo Differential Operator Technique for MCNP™

Los Alamos
NATIONAL LABORATORY

Los Alamos National Laboratory is operated by the University of California for the United States Department of Energy under contract W-7405-ENG-36.

Edited by Patricia W. Mendius, Group CIC-1
Prepared by M. Ann Nagy, Group XTM

An Affirmative Action/Equal Opportunity Employer

LA-13098

UC-705
Issued: February 1996

Verification of the Monte Carlo Differential Operator Technique for MCNP™

Gregg W. McKinney
Jess L. Iverson

Los Alamos
NATIONAL LABORATORY
Los Alamos, New Mexico 87545

VERIFICATION OF THE MONTE CARLO DIFFERENTIAL OPERATOR TECHNIQUE FOR MCNP™

by

Gregg W. McKinney and Jess L. Iverson

ABSTRACT

The differential operator perturbation technique has been incorporated into the Monte Carlo N-Particle transport code MCNP and will become a standard feature of future releases. This feature includes first and second order terms of the Taylor series expansion for response perturbations related to cross-section data (i.e., density, composition, etc.). Perturbation and sensitivity analyses can benefit from this technique in that predicted changes in one or more tally responses may be obtained for multiple perturbations in a single run. The user interface is intuitive, yet flexible enough to allow for changes in a specific microscopic cross section over a specified energy range. With this technique, a precise estimate of a small change in response is easily obtained, even when the standard deviation of the unperturbed tally is greater than the change. Furthermore, results presented in this report demonstrate that first and second order terms can offer acceptable accuracy, to within a few percent, for up to 20-30% changes in a response.

I. INTRODUCTION

Over the last few decades, users of the Monte Carlo radiation transport code MCNP[1] have expressed the need for a perturbation capability. The perturbation technique chosen for inclusion as a standard feature in future releases of MCNP is described in this report. This new MCNP feature will provide the radiation transport analyst with a powerful tool for predicting the effect of multiple perturbations within a single run.

The evaluation of response sensitivities to cross-section data involves finding the ratio of the change in response to the infinitesimal change in the data, as given by the Taylor series expansion. In deterministic methods, this ratio is approximated by performing two calculations, one with the original data and one with the perturbed data. This approach is useful even when the magnitude of the perturbation becomes very small. In Monte Carlo methods, however, this approach fails as the magnitude of the perturbation becomes small, due to the uncertainty associated with the response. For this reason, the differential operator technique was developed.

The differential operator perturbation technique as applied to the Monte Carlo method was introduced by Olhoeft[2] in the early 1960's. Nearly a decade after its introduction, this technique was applied to geometric perturbations by Takahashi.[3] A decade later, the method was generalized for perturbations in cross-section data by Hall[4,5] and later Rief.[6] A rudimentary implementation into MCNP followed shortly thereafter.[7] With an enhancement of the user interface and the addition of second order effects, this implementation has evolved into a standard MCNP feature.

Other perturbation techniques have been developed over the years, especially for use in reactivity calculations. Early on, the source correction technique was suggested by Matthes[8] and later refined by Gubbins,[9] Hoffman et al.,[10] and Matthes.[11] Also during this time, the correlated sampling technique was suggested by Matthes[8] and later refined by Kschwendt et al.,[12] Bernnat,[13] and Nakagawa et al.[14] For nearly two decades, numerous authors have used and refined these techniques. In the late 1970's, the correlated sampling technique was implemented in MCNP for fixed-source problems and used by Preeg et al.[15] Unfortunately this technique never became a permanent feature of MCNP, due in part to its impact on the code structure and its likelihood of producing unbounded variances for large perturbations.

In the following section, a theoretical overview of the differential operator technique is presented. This section begins with a derivation of the differential operator and concludes with the first and second order equations implemented in MCNP. Section III introduces the MCNP user

interface developed for the perturbation capability (i.e., PERT card). Perturbation results for an initial verification effort are provided in Section IV. This verification effort comprises the primary purpose of this report and includes a variety of test problems taken from the MCNP 4A test suite. The final section presents conclusions. The MCNP input files used in the verification effort are given in Appendix A. Appendix B provides several examples demonstrating various aspects of the MCNP perturbation feature, and Appendix C presents various statistical equations used to evaluate the perturbation results. Finally, Appendix D gives insight into applying the differential operator technique to non-standard tallies.

II. DIFFERENTIAL OPERATOR TECHNIQUE

The following section derives the generic differential operator for the n^{th} order Taylor series coefficient. The next two sections apply this operator to the Monte Carlo transport equations to obtain the first and second order coefficient estimators used in MCNP.

A. Derivation of the Operator

In the differential operator approach, a change in the Monte Carlo response c, due to changes in a related data set (represented by the parameter v), is given by a Taylor series expansion

$$\Delta c = \frac{dc}{dv} \cdot \Delta v + \frac{1}{2!} \cdot \frac{d^2c}{dv^2} \cdot \Delta v^2 + \ldots + \frac{1}{n!} \cdot \frac{d^nc}{dv^n} \cdot \Delta v^n + \ldots \ ,$$

where the n^{th} order coefficient is

$$u_n = \frac{1}{n!} \cdot \frac{d^nc}{dv^n} \ .$$

This can be written as

$$u_n = \frac{1}{n!} \sum_{b \in B} \sum_{h \in H} x_b^n(h) \left(\frac{\partial^n c}{\partial x_b^n(h)} \right) \ , \tag{1}$$

for the data set

$$x_b(h) = K_b(h) \cdot e^v; \quad b \in B, h \in H \ ,$$

where $K_b(h)$ is some constant, B represents a set of macroscopic cross sections, and H represents a set of energies or an energy interval. Note the use of the chain rule in the derivation of Eq. (1).

For a track based response estimator

$$c = \sum_j t_j q_j \ ,$$

where t_j is the response estimator and q_j is the probability of path segment j (path segment j is comprised of segment j- 1 plus the current track). Equation (1) becomes

$$u_n = \frac{1}{n!} \sum_j \left[\sum_{b \in B} \sum_{h \in H} x_b^n(h) \left(\frac{\partial^n}{\partial x_b^n(h)} (t_j q_j) \right) \right] \ ,$$

or

$$u_n = \frac{1}{n!} \sum_j \gamma_{nj} t_j q_j \ , \tag{2}$$

where

$$\gamma_{nj} \equiv \sum_{b \in B} \sum_{h \in H} x_b^n(h) \left(\frac{\partial^n}{\partial x_b^n(h)} (t_j q_j) \right) \left(\frac{1}{t_j q_j} \right) \ .$$

With some manipulations presented in Ref. 16, the path segment estimator of Eq. (2) can be converted to a particle history estimator of the form

$$u_n = \sum_i V_{ni} p_i \ ,$$

where pi is the probability of the i^{th} history and V_{ni} is the n^{th} order coefficient estimator for history i, given by

$$V_{ni} \equiv \frac{1}{n!}\sum_{j} \gamma_{nj} t_{j} \quad . \tag{3}$$

Note that this sum involves only those path segments j' in particle history i. Equation (3) shows how the history estimator for the n^{th} order coefficient can be computed from the track (or path segment) based operator Y_{nj}. The Monte Carlo expected value of u_n becomes

$$\langle u_n \rangle = \frac{1}{N}\sum_{i} V_{ni}$$

$$= \frac{1}{Nn!}\sum_{i}\left(\sum_{j} \gamma_{nj} t_{j}\right) \quad , \tag{4}$$

for a sample of N particle histories.

B. First Order

For a first order perturbation, the differential operator becomes

$$\gamma_{1j} = \sum_{b \in B}\sum_{h \in H} x_b(h)\left(\frac{1}{q_j}\right)\left(\frac{\partial q_j}{\partial x_b(h)}\right) \quad ,$$

assuming the response estimator t_j is not a function of $x_b(h)$ (see Appendix D). The path segment probability can be written as the product of track probabilities

$$q_j = \prod_{k=0}^{m} r_k \quad ,$$

where r_k is the probability of track k and segment j' contains m+l tracks. In terms of tracks, the operator becomes

$$\gamma_{1j} = \sum_{k=0}^{m}\left[\sum_{b \in B}\sum_{h \in H} x_b(h)\left(\frac{1}{r_k}\right)\left(\frac{\partial r_k}{\partial x_b(h)}\right)\right]$$

or

$$\gamma_{1j} = \sum_{k=0}^{m} \beta_{jk} \quad , \tag{5}$$

where

$$\beta_{jk} \equiv \sum_{b \in B} \sum_{h \in H} x_b(h) \left(\frac{1}{r_k}\right) \left(\frac{\partial r_k}{\partial x_b(h)}\right) \quad . \tag{6}$$

Defining track probabilities, r_k, in terms of Monte Carlo transport parameters is the final step of this derivation. If the k^{th} track starts with a neutron undergoing reaction type "a" at energy E′ and is scattered from angle θ′ to angle θ and energy E, continues for a length λ_k, and collides, then

$$r_k = \left(\frac{x_a(E')}{x_T(E')}\right) P_a(E' \rightarrow E; \theta' \rightarrow \theta)\, dE d\theta \left(e^{-x_T(E)\lambda_k}\right) x_T(E)\, d\lambda \quad , \tag{7}$$

where $x_a(E')$ is the macroscopic reaction cross section at energy E′, $x_T(E')$ is the total cross section at energy E′, and $P_a(E'->E;\theta'->\theta)dEd\theta$ is the probability distribution function in phase space of the emerging neutron. Equation (6) becomes

$$\beta_{jk} = \sum_{b \in B} \sum_{h \in H} \left(\delta_{hE}\delta_{ba} - \frac{\delta_{hE} x_b(E')}{x_T(E')} - \delta_{hE} x_b(E)\, \lambda_k + \frac{\delta_{hE} x_b(E)}{x_T(E)} \right) \quad , \tag{8}$$

where δ_{hE} and δ_{ba} are unity if h=E and b=a, otherwise they vanish. A similar derivation can be performed for other types of tracks (i.e., collision to boundary, boundary to collision, and boundary to boundary), leading to one or more of these four terms. Finally, combining Eqs. (4) and (5) gives the expected value of the first order coefficient

$$\langle u_1 \rangle = \frac{1}{N} \sum_i \left[\sum_j \left(\sum_{k=0}^{m} \beta_{jk} \right) t_j \right],$$

where $\beta_{j'k}$ is calculated from one or more terms of Eq. (8) for track k.

C. Second Order

For a second order perturbation, the differential operator becomes

$$\gamma_{2j} = \sum_{b \in B} \sum_{h \in H} x_b^2(h) \left(\frac{1}{q_j}\right) \left(\frac{\partial^2 q_j}{\partial x_b^2(h)}\right) ,$$

again assuming the response estimator $t_{j'}$ is not a function of $x_b(h)$. Omitting steps presented in Ref. 16, the second order operator becomes

$$\gamma_{2j} = \sum_{k=0}^{m} (\alpha_{jk} - \beta_{jk}^2) + \left(\sum_{k=0}^{m} \beta_{jk}\right)^2 ,$$

where

$$\alpha_{jk} \equiv \sum_{b \in B} \sum_{h \in H} x_b^2(h) \left(\frac{1}{r_k}\right) \left(\frac{\partial^2 r_k}{\partial x_b^2(h)}\right) .$$

It is evident that $\gamma_{2j'}$ requires little additional effort to $\gamma_{1j'}$, namely the computation of $\alpha_{j'k}$. If r_k is given by Eq. (7), then $\alpha_{j'k}$ becomes

$$\alpha_{jk} = \sum_{b \in B} \sum_{h \in H} \left(\frac{2\delta_{hE} x_b^2(E')}{x_T^2(E')} - \frac{2\delta_{hE}\delta_{ba} x_b(E')}{x_T(E')} + \delta_{hE} x_b^2(E) \lambda_k^2 - \frac{2\delta_{hE} x_b^2(E) \lambda_k}{x_T(E)} \right) . \qquad (9)$$

Once again, for other types of tracks one or more of these four terms is required. The expected value of the second order coefficient, via Eq. (4), becomes

$$\langle u_2 \rangle = \frac{1}{2N} \sum_i \left[\sum_j \left(\sum_{k=0}^{m} (\alpha_{jk} - \beta_{jk}^2) + \left(\sum_{k=0}^{m} \beta_{jk} \right)^2 \right) t_j \right] ,$$

where $\beta_{j'k}$ is given by one or more terms of Eq. (8) and $\alpha_{j'k}$ by one or more terms of Eq. (9) for track k.

III. MCNP USER INTERFACE

The perturbation user interface is described in the following two sections. This interface is intuitive, requiring a minimum of input, and yet flexible enough to allow for changes in a specific microscopic cross section over a specified energy range.

A. General Description

The PERT card allows the user to make perturbations in cell material density, composition, or cross-section data. Using the differential operator technique, the perturbation estimates are made without actually changing the input material specifications. Multiple perturbations can be applied in the same run, each specified by a separate PERT card. There is no limit to the number of perturbations, since dynamic memory is used for perturbation storage. The entire tally output is repeated for each perturbation, giving the estimated differential change in the tally or, alternately, this change added to the unperturbed tally (see the METHOD keyword). Perturbations to the k_{eff} estimator can be made by use of a track-length tally estimate of k_{eff}. The CELL keyword and either the MAT or RHO keyword are required.

Form: **PERTn:pl keyword=parameter(s) keyword=parameter(s) ...**

n = Unique, arbitrary perturbation number.

pl = N or P or N,P. Not available for electrons.

keyword = See the following section.

B. PERT Card Keywords

Six keywords are currently available for the PERT card. The CELL keyword and either the MAT or RHO keyword are required. The METHOD, ERG, and RXN keywords invoke more advanced options. These keywords are described below:

CELL - The one or more entries following this keyword indicate which cells are perturbed. At least one entry is required, and there is no limit to the number of entries. A comma or space delimiter is required between entries:

CELL=1,2,3,4

CELL=1 10i 12

MAT - The entry following this keyword specifies the perturbation material number, which must have a corresponding M card. Composition changes can only be made through the use of this keyword. If the RHO keyword is omitted, this keyword is required. Note in the following section that certain composition changes are prohibited.

RHO - Specifies the perturbed density of the cell(s) listed after the CELL keyword. A positive entry indicates units of atoms/barn-cm and a negative entry grams/cm^3. If the MAT keyword is omitted, this keyword is required.

METHOD - This keyword specifies the number of terms to include in the perturbation estimate:

1 - include first and second order (default)

2 - include only first order

3 - include only second order

A positive entry produces perturbation tallies which give the estimated *differential* change in the unperturbed tally (default). A negative entry generates perturbation tallies such that this change is *added* to the unperturbed tally. The ability to produce first and second order terms separately enables the user to determine the significance of including the second-order estimator for subsequent runs. If the second-order results are a significant fraction (20%) of the total, then higher order terms are necessary to accurately predict the change in the unperturbed tally. In such cases, the magnitude of the perturbation should be reduced to satisfy this condition. Typically, this technique is accurate to within a few percent for up to 30% changes in the unperturbed tally.

ERG - The two entries following this keyword specify an energy range in which the perturbation is applied. The default range includes all energies. This keyword is usually used with the RXN keyword to perturb a specific cross section over a particular energy range.

RXN - The one or more entries following this keyword must be ENDF/B reaction types that identify one or more cross sections to perturb. A list of

available reaction types is given in Appendix G of Ref. 1. This keyword allows the user to perturb a specific cross section of a single nuclide in a material, as well as to perturb a set of cross sections for all nuclides in a material. See the examples in Appendix B.

C. Limitations

Although it is always a high priority to minimize the limitations of any MCNP feature, the perturbation technique itself, in addition to the numerous other MCNP features, resulted in the following limitations:

1. A fatal error is generated if a PERT card attempts to unvoid a region. The simple solution is to include the material in the unperturbed problem and void the region of interest with the PERT card (see Appendix B for more details).
2. A fatal error is generated if a PERT card attempts to alter a material composition in such a way as to introduce a new nuclide, The solution is to set up the unperturbed problem with a mixture of both materials and introduce PERT cards to remove each (see Appendix B for more details).
3. Exercise caution when using a PERT card with FM tallies. If the perturbed cross section is also listed on an FM tally, the estimated change in that tally is likely invalid, due to an additional term that has not yet been implemented (see Appendix D). For example, if the FM tally is a track-length k_{eff} estimator and the perturbation is a change in density of the fissile material, then the perturbation estimate will be invalid since both the tally and perturbation involve the fission cross section. In most cases this term can be determined with an additional FM tally.
4. DXTRANs and point detector tallies are not currently compatible with the PERT card. This limitation may be removed in future versions.
5. While there is no limit to the number of perturbations, they should be kept to a minimum, as each perturbation can degrade performance by 1O-2O%.

D. Examples

The following examples demonstrate some basic features of the PERT card. See Appendix B for detailed examples of voiding and unvoiding regions, composition and geometric perturbations, and sensitivity estimates.

1. First Example.

```
1     1   .05   -1 2 –3 4 -5 6 $ Material 1 at .05 atoms/barn–cm
```

PERT1:n,p CELL=l RHO=0.03

This PERT card specifies a density change from .05 to .03 atoms/barn-cm in cell 1. Note that this perturbation is applied to both neutron and photon interactions, therefore perturbation results will be generated for both neutron and photon tallies. In a coupled neutron and photon problem, a change applied only to neutrons (e.g., PERT1:n) can still produce changes in a photon tally.

2. Second Example.

```
4     1   -1.   - 1 2 - 3 4 - 5 6          $ Material 1 at 1 g/cm3
5     1   -1.   -7 8 -9 10 -11 12          $ Material 1 at 1 g/cm3


Ml   1001  .333334  1002 .333333 8016 .333333   $Water Mixture
M8               1002 .666667 8016 .333333   $ Heavy water
```

PERT2:n CELL=4,5 MAT=8 RHO=-1.2

This perturbation changes the material composition of cells 4 and 5 from material 1 to material 8. The MAT keyword on the PERT card specifies the perturbation material. Note that the material density is also changed from 1.0 to 1.2 g/cm^3.

3. Third Example. .

PERT3:n,p CELL=l 10i 12 RHO=O. METHOD=-1

This PERT card simply voids cells 1 through 12 for both neutrons and photons. Note that the predicted changes will be added to the unperturbed tallies (i.e., METHOD=- 1).

IV. VERIFICATION RESULTS

The perturbation results presented in the following sections involve ten test problems taken from the MCNP 4A test suite. This initial verification effort differs from a benchmark in that experimental results are not available for comparison. The primary purpose of this effort is to verify the implementation of the differential operator perturbation technique in MCNP. To this end, a variety of test problems were chosen for inclusion in this report: five neutron fixed-source problems, one photon fixed-source problem, two coupled neutron/photon fixed-source problems, and two criticality problems. The intermediate 4XP version of MCNP was used to generate these perturbation results.

In each of these test problems, four perturbations were investigated, corresponding to approximately 5%, 10%, 20%, and 30% changes in a relevant tally. The 30% upper bound was chosen to verify the relevance and range of applicability of the second order term. The 5% lower bound was chosen to limit the execution time needed to determine the tally changes based on separate runs. Except where noted, a relevant tally was identified from among the existing tallies in the original input file. The tally results reported in this section are generally that for the total bin.

Five perturbation input files were generated for each test problem. In the first, the original input file was modified to include four PERT cards, one for each perturbation as discussed above. This input file produced the predicted change in the relevant tally for each of the four PERT cards. In each of the remaining four input files, the original input file was modified to include the actual perturbation prescribed on the corresponding PERT card. These files produced the actual change in the relevant tally. The perturbation input files are included in Appendix A to remove any ambiguity of the problem descriptions.

A. Neutron Fixed-Source Problems

The five fixed-source neutron problems are discussed in the following sections. Each section includes a short description of the geometry followed by a discussion of the actual and predicted perturbation results.

1. Test Problem INP01. Input file INP01 consists of an inner sphere of graphite surrounded by a spherical shell of copper (see Fig. 1). There is an isotropic point source at the center of the graphite sphere with a uniform energy spectrum from 1 to 14.1 MeV.

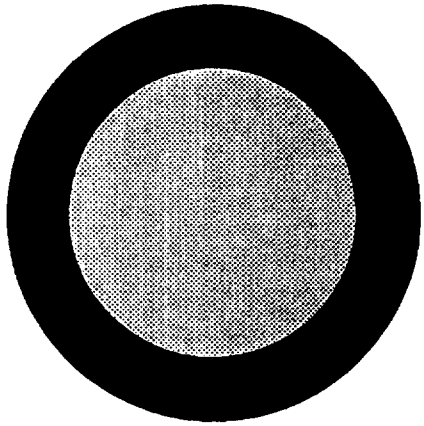

Fig. 1. Geometry plot of test problem INP01.

Tally 1 calculates the relative neutron current across the surface of the graphite sphere, adjusted by energy and cosine multipliers. Results for the last cosine bin and total energy bin are reported below. The density of the graphite was reduced from 2.25 g/cm^3 to 1.85, 1.40, 0.60, and .005 g/cm^3, the latter of which increased Tally 1 by nearly 30%. Table I gives the actual and predicted changes to Tally 1 along with their relative errors. The actual differential change is obtained by subtracting the perturbed and unperturbed results, whereas the predicted change, produced by the PERT card, gives the differential change directly. These differential changes were normalized by the unperturbed tally to give the percent change in Tally 1. Table I lists the actual percent increase as 5.02%, 10.38%, 20.36%, and 28.58% for the four graphite perturbations and the predicted percent increase as 4.75%, 10.28%, 20.59%, and 28.65%. In both cases, the tabulated relative errors were calculated by standard propagation of error formulas given in Appendix C. Figure 2 plots these results as a function of the differential decrease in graphite density. When plotted in this manner, a straight line represents a perturbation that can be accurately estimated with only the first order term. As evident from Fig. 2, the PERT card accurately predicts the change in Tally 1, even up to a 30% change. While the relative errors of both the actual and predicted results are small, their trends are significant. For the actual change, the relative error *increases* with smaller perturbations — in fact it is unbounded as the perturbation goes to zero. However, for the predicted change, the relative error increases gradually with larger perturbations and *decreases* with smaller perturbations. This effect is more pronounced in subsequent test problems.

TABLE I
ACTUAL AND PREDICTED PERTURBATION RESULTS FOR TALLY 1 OF PROBLEM INP01.

	Graphite Density (g/cm^3)=	2.250	1.850	1.400	0.600	0.005
Actual	Current (# n)	6.0035E1	6.3048E1	6.6265E1	7.2258E1	7.7191E1
	Relative Error	0.0015	0.0030	0.0029	0.0027	0.0026
	% Change		5.02%	10.38%	20.36%	28.58%
	Relative Error		0.0695	0.0341	0.0176	0.0129
Predicted	Current Change		2.8544E0	6.1743E0	1.2361E1	1.7198E1
	Relative Error		0.0059	0.0062	0.0069	0.0075
	% Change		4.75%	10.28%	20.59%	28.65%
	Relative Error		0.0061	0.0064	0.0071	0.0076

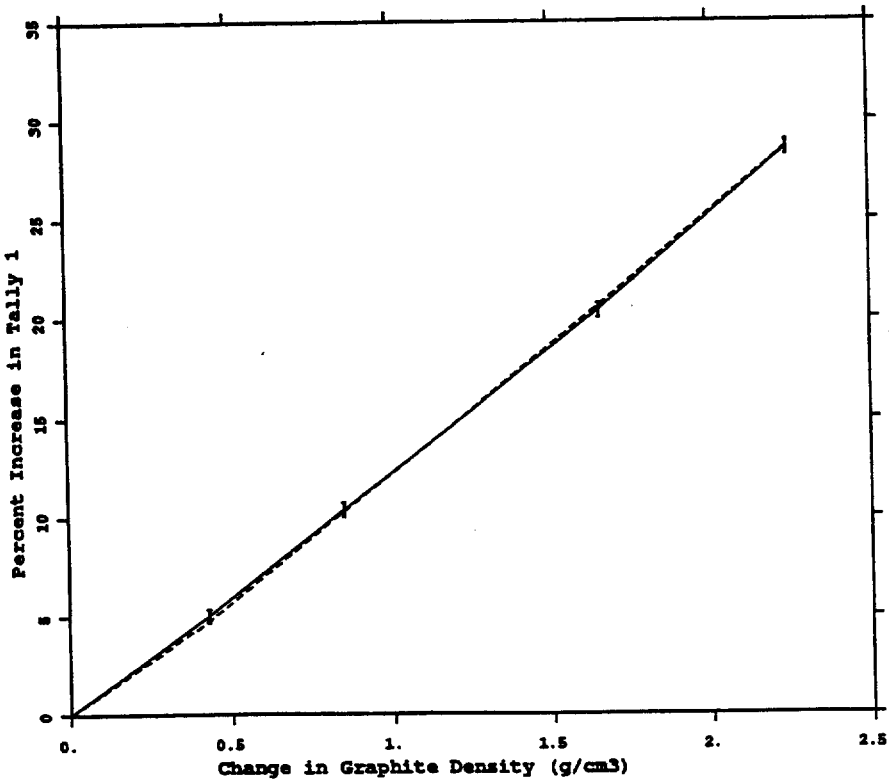

Fig. 2. Change in Tally 1 of problem INP01 due to a decrease in the graphite density. Solid line is Actual and dashed line is Predicted.

2. Test Problem INP02. As in the previous problem, input file INP02 involves a simple geometric model consisting only of spheres (see Fig. 3). The large set of spheres include an inner region of boron surrounded by an aluminum shell. Within this aluminum shell, is another set of spheres filled with aluminum. The source is distributed within the boron sphere and has a uniform energy spectrum from 0.1 to 1.0 MeV. Note, the input file used for this test problem was further modified to disable the DXTRAN feature (see Appendix A).

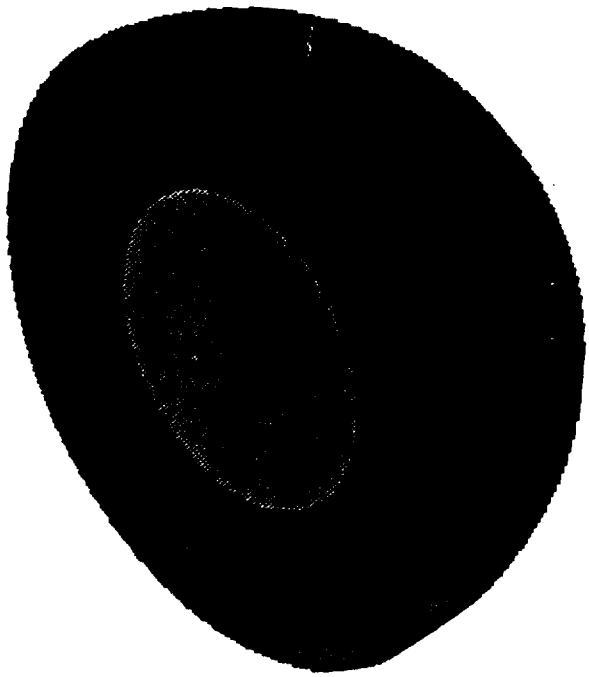

Fig. 3. Geometry plot of test problem INP02.

Tally 1, which calculates the current across the boron-aluminum interface, was chosen as the tally of interest for this problem. The boron composition was perturbed from a ^{10}B atom fraction of .196 to a value of .250, .325, .510, and .720. Table II shows the corresponding decrease in Tally 1 of 5.47%, 10.56%, 21.46%, and 31.15% for the actual change and 4.59%, 10.32%, 21.11%, and 27.65% for the predicted change. Figure 4 plots these results as a function of the differential increase in ^{10}B atom fraction. The nonlinearity of these curves indicates the importance of including the second order term. This issue is discussed further in Section IV.E.

TABLE III
ACTUAL AND PREDICTED PERTURBATION RESULTS FOR TALLY 7 OF PROBLEM INP07

	UO_2 Density (g/cm^3)=	8.1	8.8	9.2	10.3	11.5
Actual	Energy (MeV/g)	7.1762E-3	7.5546E-3	7.8774E-3	8.6556E-3	9.6147E-3
	Relative Error	0.0069	0.0068	0.0075	0.0075	0.0080
	% Change		5.27%	9.77%	20.62%	33.98%
	Relative Error		0.1887	0.1102	0.0556	0.0381
Predicted	Energy Change		4.1825E-4	6.6828E-4	1.3973E-3	2.2618E-3
	Relative Error		0.0344	0.0358	0.0396	0.0438
	% Change		5.83%	9.31%	19.47%	31.52%
	Relative Error		0.0351	0.0365	0.0402	0.0443

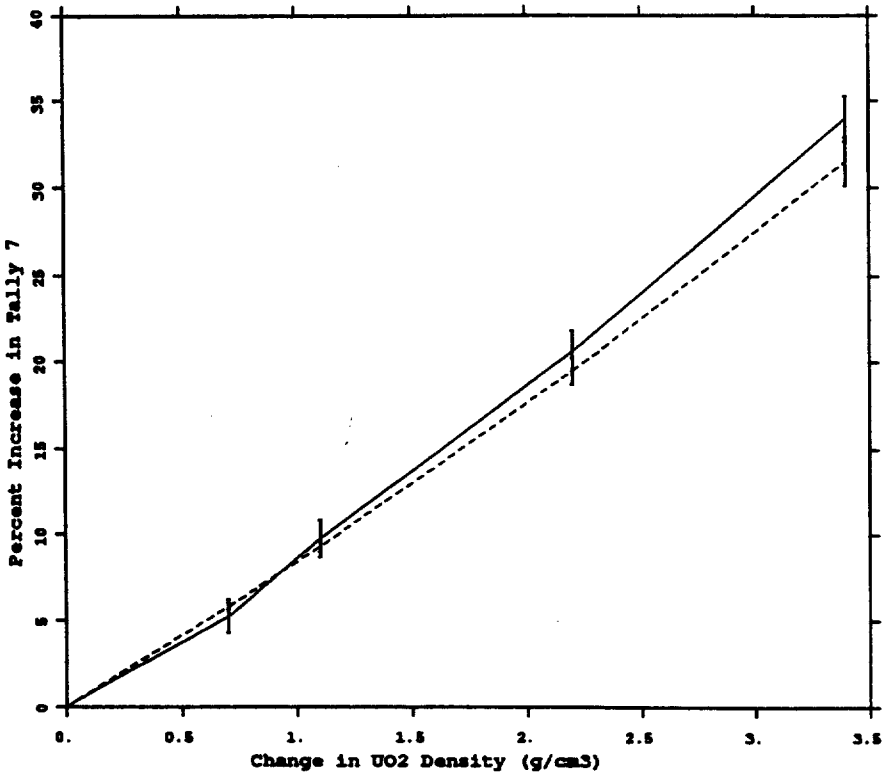

Fig. 6. Change in Tally 7 of problem INP07 due to an increase in the UO_2 density. Solid line is Actual and dashed line is Predicted.

4. Test Problem INP12. Input file INP12 involves a much more complex geometric model. This model includes an oil-well logging tool positioned in a borehole within a limestone formation (see Fig. 7). The tool consists of an americium/beryllium neutron source (dark cylinder on the left) and two helium detectors (light cylinders on the right) embedded within a cylindrical region of iron. Water fills the cylindrical borehole between the tool and formation. The neutron source is directed radially into the limestone and ranges in energy from a few keV to 11 MeV.

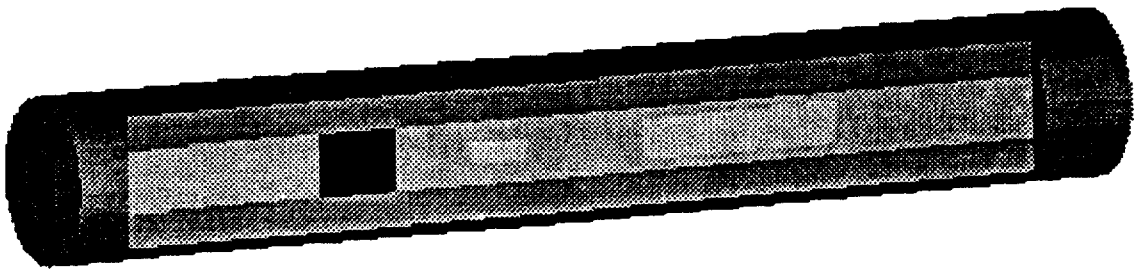

Fig. 7. Geometry plot of test problem INP12.

Tally 44, which gives the absorption rate in the far detector, was chosen as the tally of interest for this problem. The iron density of the tool was decreased from 7.86 g/cm^3 to 7.72, 7.48, 7.17, and 6.84 g/cm^3. Table IV gives the corresponding increase in Tally 44 of 5.88%, 10.45%, 20.91%, and 30.19% for the actual change and 3.54%, 9.97%, 18.91%, and 29.24% for the predicted change. As discussed in Section IV.A.1, the difference in related relative errors associated with these percent changes can be notable. The first perturbation in Table IV demonstrates this with a 19.24% relative error associated with the actual percent change and only a 0.88% relative error associated with the predicted percent change. As the relative error associated with an actual run (e.g., 0.98% for the first perturbation) approaches the magnitude of the percent change (e.g., 5.88% for the first perturbation), the relative error associated with the percent change becomes large. Figure 8 plots these results as a function of the differential increase in iron density. Once again, these curves show good agreement within the reported one-sigma statistical uncertainties.

TABLE IV
ACTUAL AND PREDICTED PERTURBATION RESULTS FOR TALLY 44 OF PROBLEM INP12

	Iron Density (g/cm^3)=	7.86	7.72	7.48	7.17	6.84
Actual	Flux (n/cm2)	1.7191E-4	1.8202E-4	1.8987E-4	2.0785E-4	2.2381E-4
	Relative Error	0.0045	0.0098	0.0096	0.0094	0.0090
	% Change		5.88%	10.45%	20.91%	30.19%
	Relative Error		0.1924	0.1103	0.0586	0.0418
Predicted	Flux Change		6.0912E-6	1.7132E-5	3.2513E-5	5.0273E-5
	Relative Error		0.0076	0.0078	0.0081	0.0084
	% Change		3.54%	9.97%	18.91%	29.24%
	Relative Error		0.0088	0.0090	0.0093	0.0095

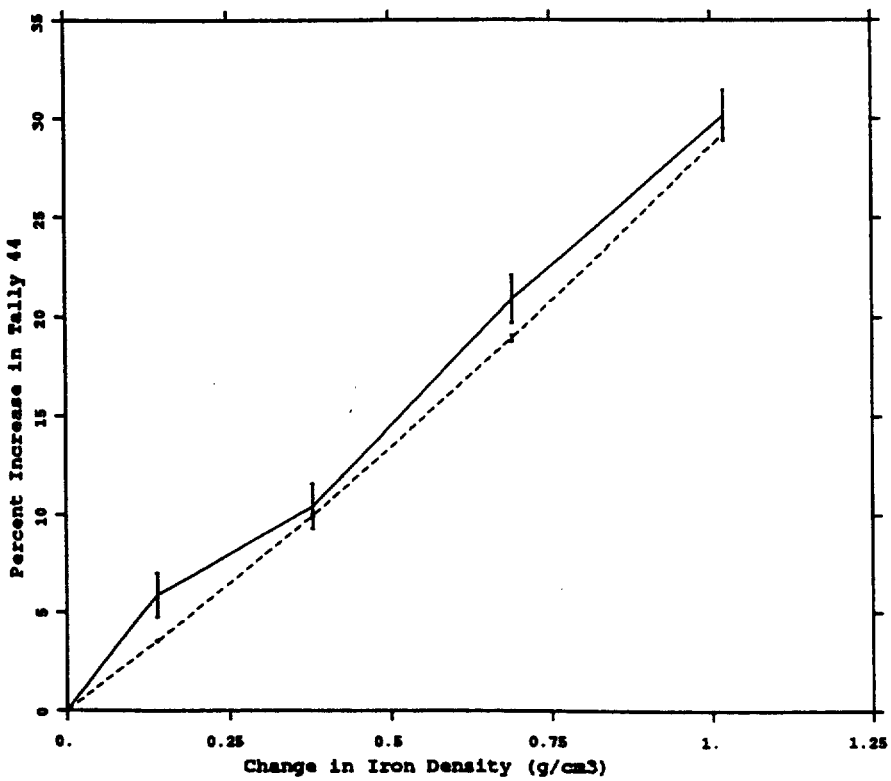

Fig. 8. Change in Tally 44 of problem INP12 due to a decrease in the iron density. Solid line is Actual and dashed line is Predicted.

5. Test Problem INP14. Input file INP14 consists of five repeated units within a sphere of carbon (see Fig. 9). Each of these five cubes is filled with ^{235}U and three rod containers. Each rod container includes four ^{235}U rods surrounded by carbon. A neutron source is distributed uniformly in each of the ^{235}U rods with an energy range of 1-11 MeV.

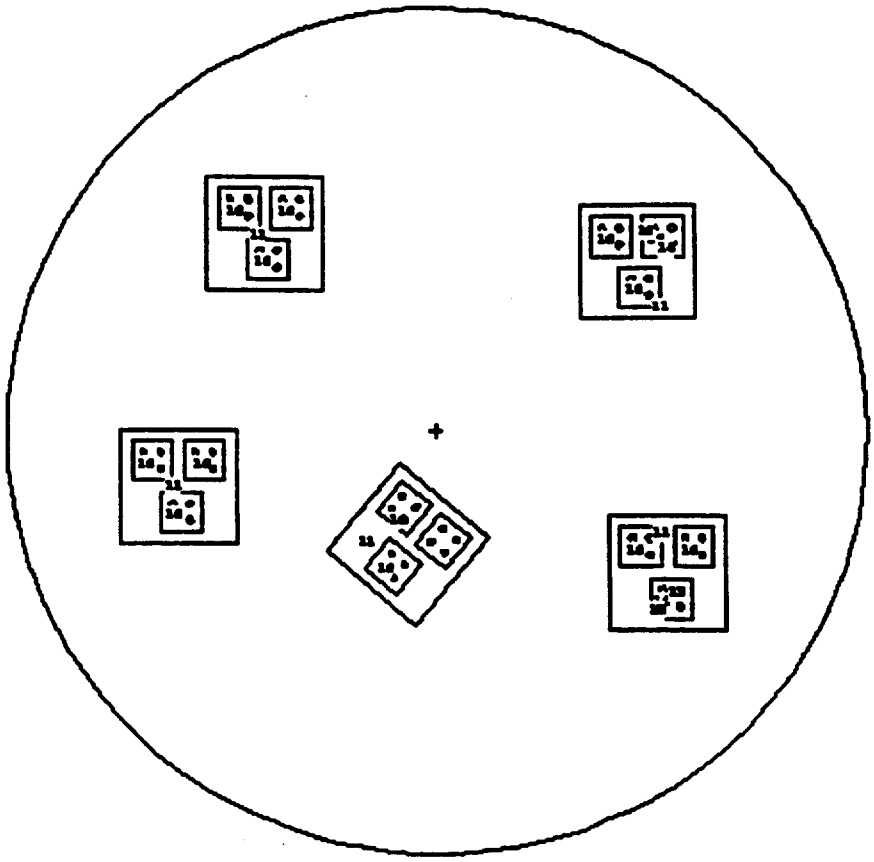

Fig. 9. Geometry plot of test problem INP14.

The first tally bin of Tally 4 calculates the neutron flux averaged over the first ^{235}U rod in each of the 15 rod containers and was chosen as the tally of interest for this problem. The carbon density, within both the rod containers and the large sphere, was increased from 0.5 g/cm^3 to 1.0, 1.7, 3.5, and 6.0 g/cm^3. Table V gives the corresponding increase in Tally 4 of 4.46%, 10.54%, 20.30%, and 30.13% for the actual change and 3.50%, 8.63%, 23.16%, and 46.45% for the predicted change. Figure 10 plots these results as a function of the differential increase in carbon

density. In this case, it is evident that the first and second order terms are adequate for only up to 15-20% changes in Tally 4. Even below this value, the quadratic shape of the predicted curve does not appear to be a good match with that of the actual, though the data points are nearly within the reported statistical uncertainties.

TABLE V
ACTUAL AND PREDICTED PERTURBATION RESULTS FOR TALLY 4 OF PROBLEM INP14.

	Carbon Density (g/cm^3)=	0.5	1.0	1.7	3.5	6.0
Actual	Flux (n/cm2)	2.5452E-2	2.6587E-2	2.8134E-2	3.0620E-2	3.3121E-2
	Relative Error	0.0008	0.0121	0.0123	0.0120	0.0121
	% Change		4.46%	10.54%	20.30%	30.13%
	Relative Error		0.2840	0.1293	0.0712	0.0523
Predicted	Flux Change		8.8969E-4	2.1975E-3	5.8936E-3	1.1823E-2
	Relative Error		0.0117	0.0191	0.0380	0.0608
	% Change		3.50%	8.63%	23.16%	46.45%
	Relative Error		0.0117	0.0191	0.0380	0.0608

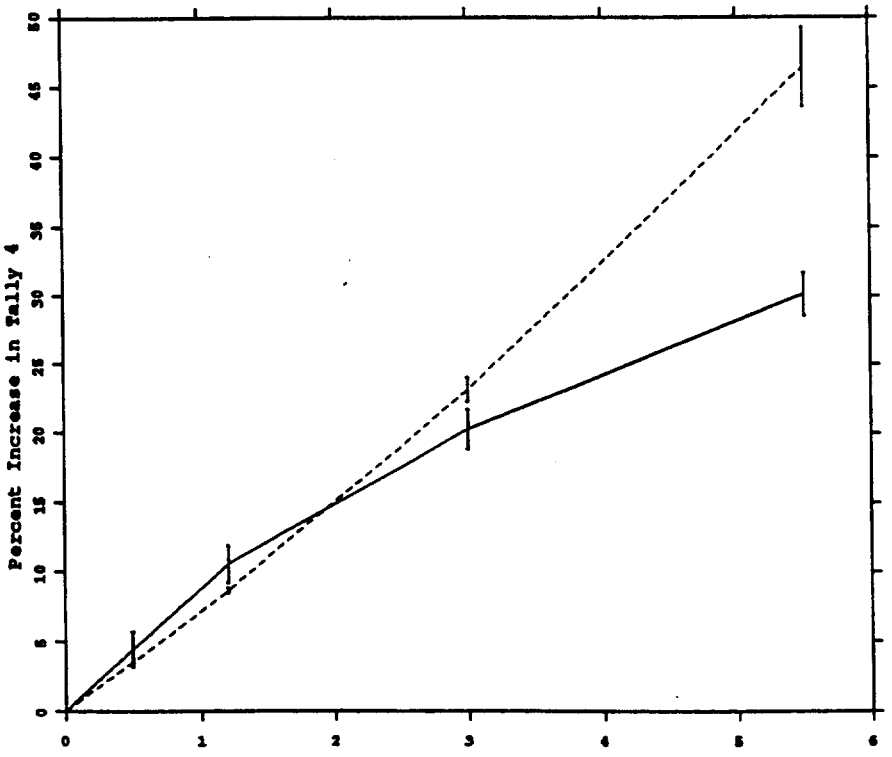

Fig. 10. Change in Tally 4 of problem INP14 due to an increase in the carbon density. Solid line is Actual and dashed line is Predicted.

B. Photon Fixed-Source Problem

One fixed-source photon problem was chosen for inclusion in this report. The following section includes a short description of the geometry followed by a discussion of the actual and predicted perturbation results.

1. Test Problem INP04. Input file INP04 consists of three sets of concentric spheres (one of each set is shown in Fig. 11). The inner sphere of the largest set is filled with UH_3, and the outer spherical shell is filled with ULi_3. The smaller sets of spheres are contained within the outer spherical shell of the largest set. Both the inner and outer layers of these smaller spheres are filled with ULi_3. A 3 MeV point source is located at the center of the largest set of spheres. Note that the input file used for this test problem was further modified to disable the DXTRAN feature (see Appendix A).

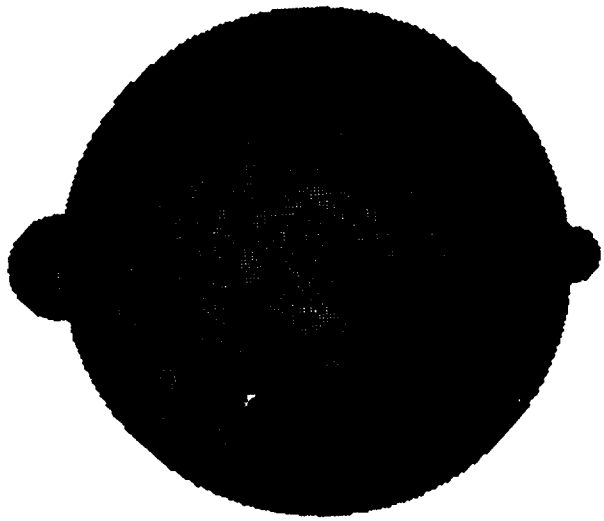

Fig. 11. Geometry plot of test problem INP04.

Tally 6, which gives the energy deposition in several materials, was chosen as the tally of interest for this problem. Results for cell 1 (UH_3) and the total energy bin are reported below. The UH_3 atom density was increased from 0.02 atoms/barn-cm to 0.0235, 0.0270, 0.035, and 0.04 atoms/barn-cm. Table VI gives the corresponding decrease in Tally 6 of 4.69%, 9.17%, 18.52%, and 23.62% for the actual change and 4.73%, 9.30%, 19.09%, and 24.75% for the predicted change. Figure 12 plots these results as a function of the differential increase in UH_3 atom density.

As expected for a nearly linear dependence, these curves show good agreement within the reported one-sigma statistical uncertainties.

TABLE VI
ACTUAL AND PREDICTED PERTURBATION RESULTS FOR TALLY 6 OF PROBLEM INP04

	UH_3 Atom Density=	0.0200	0.0235	0.0270	0.035	0.04
Actual	Energy (MeV/g)	1.7097E-4	1.6296E-4	1.5529E-4	1.3931E-4	1.3059E-4
	Relative Error	0.0019	0.0024	0.0026	0.0030	0.0033
	% Change		-4.69%	-9.17%	-18.52%	-23.62%
	Relative Error		0.0635	0.0331	0.0168	0.0135
Predicted	Energy Change		-8.0916E-6	-1.5893E-5	-3.2632E-5	-4.2323E-5
	Relative Error		0.0157	0.0143	0.0127	0.0133
	% Change		-4.73%	-9.30%	-19.09%	-24.75%
	Relative Error		0.0158	0.0144	0.0128	0.0134

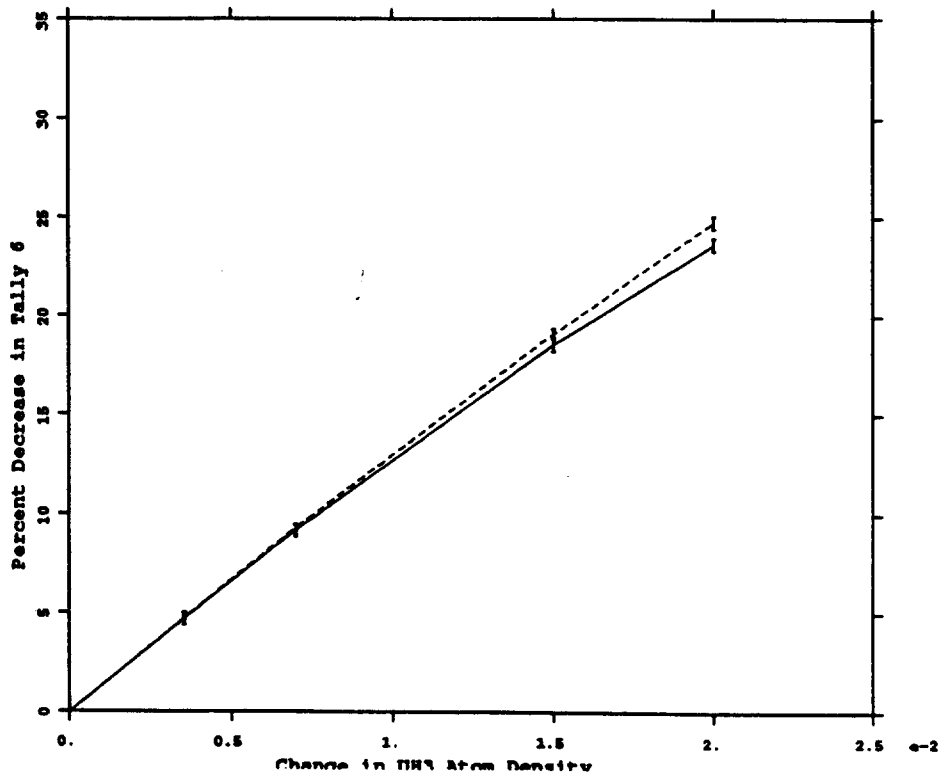

Fig. 12. Change in Tally 6 of problem INP04 due to an increase in the UH_3 atom density. Solid line is Actual and dashed line is Predicted.

C. Coupled Neutron/Photon Fixed-Source Problems

The two fixed-source coupled neutron/photon problems are discussed in the following sections. Each section includes a short description of the geometry followed by a discussion of the actual and predicted perturbation results.

1. Test Problem INP10. Input file INP10 consists of two infinite concentric cylinders, where the inner cylinder is filled with water and the outer cylindrical shell is filled with copper. Near the origin, the inner cylindrical region is cut axially into seven cylindrical disks which are filled with, from left to right in Fig. 13, water, carbon, void, water, carbon, water, and water. The void disk at the center contains a cube of CuO, and the water disk next to it contains a large void torus surrounded by a shell of copper. A neutron source is distributed uniformly in the cube of CuO and has an energy distribution given by the Watt fission spectrum.

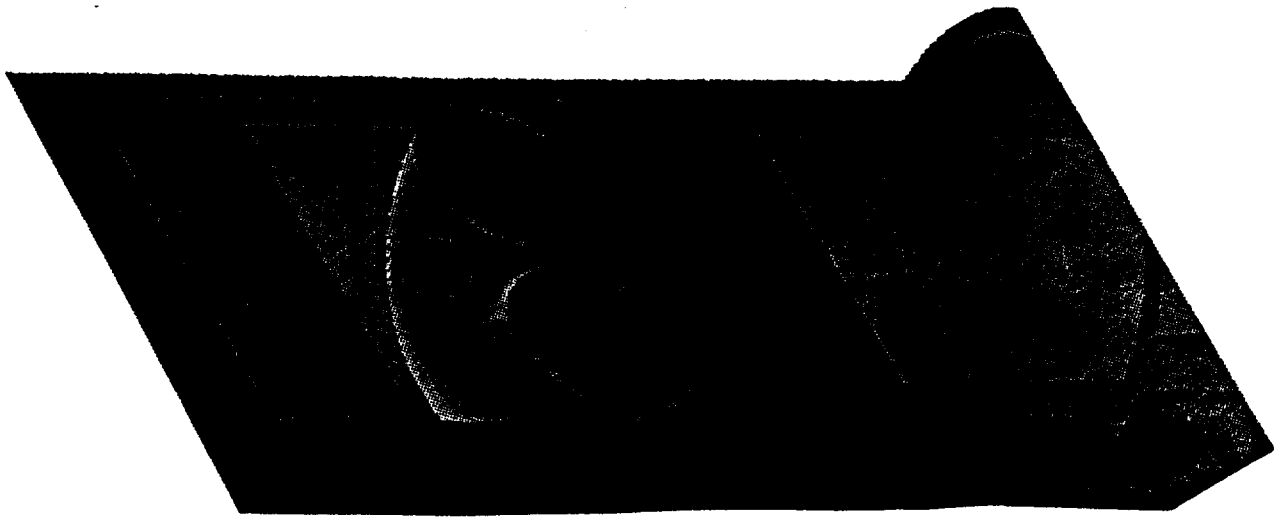

Fig. 13. Geometry plot of test problem INP10.

The last tally bin of Tally 4 gives the neutron flux averaged over the last segment of the right carbon disk and was chosen as the neutron tally of interest for this problem. A second tally of interest, Tally 14, gives the photon flux averaged over this same region. The copper density, surrounding both the infinite cylinder and the torus, was decreased from 8.94 g/cm^3 to 7.9, 6.9, 3.5, and 1.0 g/cm^3. Table VII gives the corresponding increase in Tally 4 of 4.82%, 7.80%, 20.43%, and 28.09% for the actual change and 3.99%, 7.79%, 20.45%, and 29.51% for the predicted

change. Similarly, Table VIII gives the corresponding increase in Tally 14 of 5.82%, 11.51%, 28.10%, and 4.41% for the actual change and 6.04%, 12.13%, 34.97%, and 53.84% for the predicted change. Figures 14 and 15 plot these results as a function of the differential decrease in copper density. In Fig. 14, it is evident that the predicted and actual curves are within the reported statistical uncertainties, even at the 30% data point. However, in Fig. 15 this is true only for changes up to 20%. Beyond this point, Tally 14 deviates significantly from a quadratic shape which accounts for the poor prediction at the 30% data point.

TABLE VII
ACTUAL AND PREDICTED PERTURBATION RESULTS FOR TALLY 4 OF PROBLEM INP10

	Copper Density (g/cm3)=	8.94	7.90	6.90	3.50	1.00
Actual	Flux (n/cm2)	3.1079E-5	3.2577E-5	3.3503E-5	3.7427E-5	3.9810E-5
	Relative Error	0.0033	0.0091	0.0088	0.0084	0.0080
	% Change		4.82%	7.80%	20.43%	28.09%
	Relative Error		0.2094	0.1288	0.0522	0.0385
Predicted	Flux Change		1.2403E-6	2.4218E-6	6.3571E-6	9.1702E-6
	Relative Error		0.0266	0.0303	0.0495	0.0665
	% Change		3.99%	7.79%	20.45%	29.51%
	Relative Error		0.0268	0.0305	0.0496	0.0666

TABLE VIII
ACTUAL AND PREDICTED PERTURBATION RESULTS FOR TALLY 14 OF PROBLEM INP10

	Copper Density (g/cm^3)=	8.94	7.90	6.90	3.50	1.00
Actual	Flux (n/cm2)	1.9799E-5	2.0952E-5	2.2078E-5	2.5363E-5	2.0673E-5
	Relative Error	0.0032	0.0083	0.0081	0.0074	0.0076
	% Change		5.82%	11.51%	28.10%	4.41%
	Relative Error		0.1606	0.0833	0.0357	0.1939
Predicted	Flux Change		1.1956E-6	2.4022E-6	6.9232E-6	1.0660E-5
	Relative Error		0.0215	0.0242	0.0380	0.0487
	% Change		6.04%	12.13%	34.97%	53.84%
	Relative Error		0.0217	0.0244	0.0381	0.0488

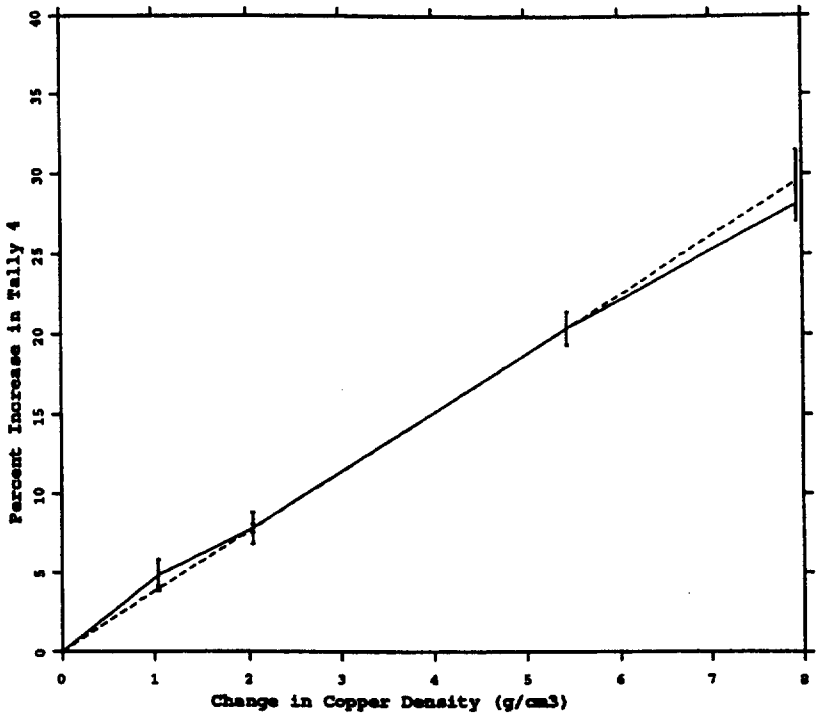

Fig. 14. Change in Tally 4 of problem INP10 due to a decrease in the copper density. Solid line is Actual and dashed line is Predicted.

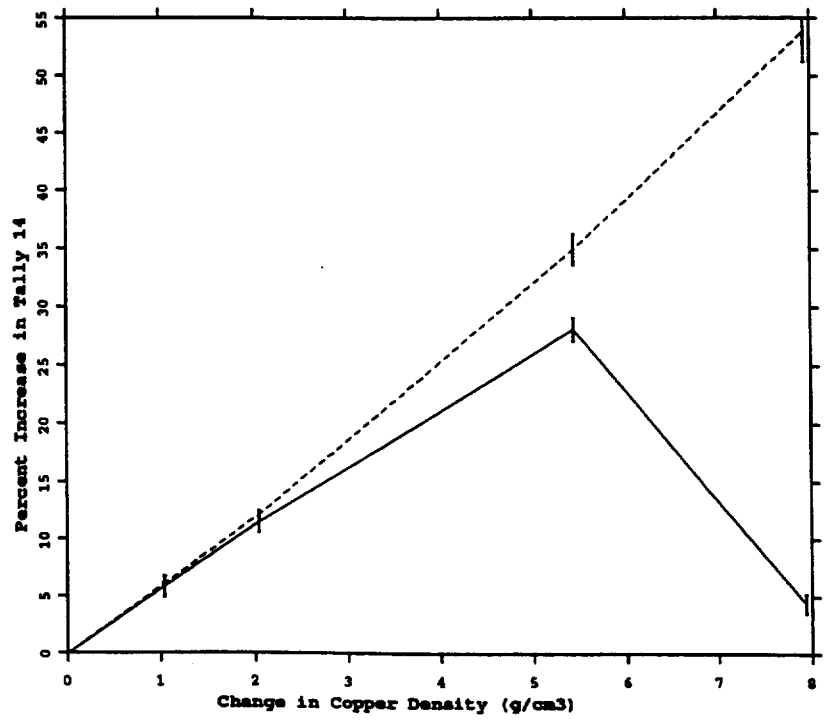

Fig. 15. Change in Tally 14 of problem INP10 due to a decrease in the copper density. Solid line is Actual and dashed line is Predicted.

2. Test Problem INP11. Input file INP11 includes a complex geometry with many odd shapes (see Fig. 16). A pretzel-shaped set of three tori filled with ^{235}U is centered at the origin. Traversing through these tori is a cage made of ellipsoids filled with SiO_2. Four "toys" of unique shape are arranged around the perimeter, each made of copper. All these objects are encased in a sphere of water. A disk-shaped, monodirectional neutron source is located in front of the tori within the water. The source energy distribution is uniform from .01 eV to 1 keV.

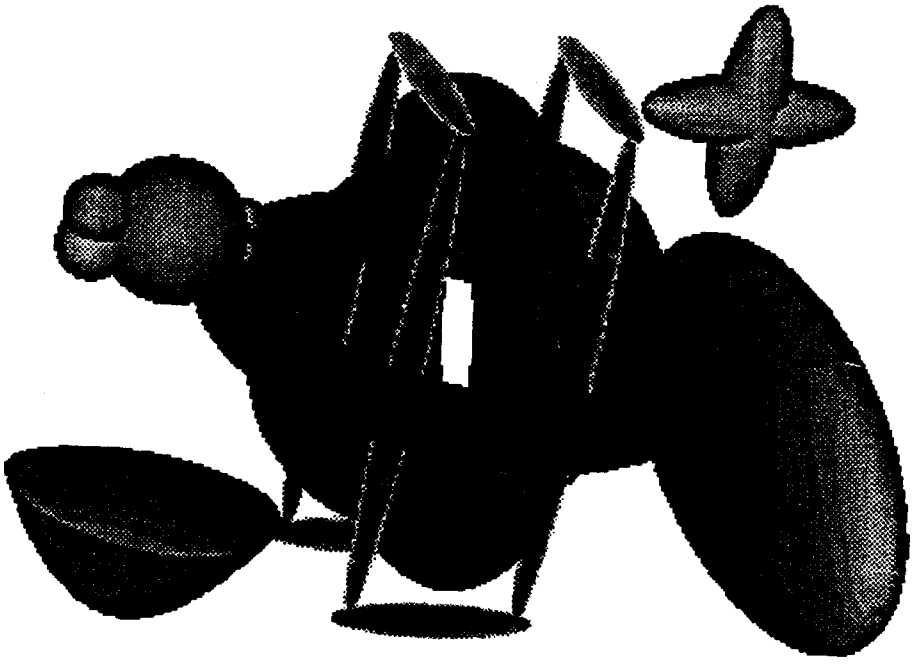

Fig. 16. Geometry plot of test problem INP11.

The first tally bin of Tally 4 gives the neutron flux averaged over the three tori and was chosen as the neutron tally of interest for this problem. A second tally of interest, Tally 11, gives the photon current across the tori surfaces. The ^{235}U density within the three tori was increased from 7.8 g/cm^3 to 8.75, 9.5, 10.9, and 12.0 g/cm^3. Table IX gives the corresponding increase in Tally 4 of 5.82%, 10.83%, 22.68%, and 30.81% for the actual change and 5.45%, 10.25%, 20.40%, and 29.44% for the predicted change. Similarly, Table X gives the corresponding increase in Tally 11 of 1.37%, 1.92%, 7.97%, and 9.56% for the actual change and 1.49%, 3.09%, 7.03%, and 11.02%

for the predicted change. Figures 17 and 18 plot these results as a function of the differential increase in ^{235}U density. Both of these sets of curves show good agreement within the reported one-sigma statistical uncertainties.

TABLE IX
ACTUAL AND PREDICTED PERTURBATION RESULTS FOR TALLY 4 OF PROBLEM INP11

	235U Density (g/cm3)=	7.80	8.75	9.50	10.90	12.00
Actual	Flux (n/cm2)	1.7264	1.8268	1.9133	2.1179	2.2583
	Relative Error	0.0022	0.0158	0.0160	0.0170	0.0179
	% Change		5.82%	10.83%	22.68%	30.81%
	Relative Error		0.2900	0.1651	0.0925	0.0764
Predicted	Flux Change		0.094105	0.17702	0.3521	0.5083
	Relative Error		0.0118	0.0124	0.0138	0.0149
	% Change		5.45%	10.25%	20.40%	29.44%
	Relative Error		0.0120	0.0126	0.0140	0.0151

TABLE X
ACTUAL AND PREDICTED PERTURBATION RESULTS FOR TALLY 11 OF PROBLEM INP11

	235U Density (g/cm3)=	7.80	8.75	9.50	10.90	12.00
Actual	Flux (n/cm2)	1.7264	1.8268	1.9133	2.1179	2.2583
	Relative Error	0.0022	0.0158	0.0160	0.0170	0.0179
	% Change		5.82%	10.83%	22.68%	30.81%
	Relative Error		0.2900	0.1651	0.0925	0.0764
Predicted	Flux Change		0.094105	0.17702	0.3521	0.5083
	Relative Error		0.0118	0.0124	0.0138	0.0149
	% Change		5.45%	10.25%	20.40%	29.44%
	Relative Error		0.0120	0.0126	0.0140	0.0151

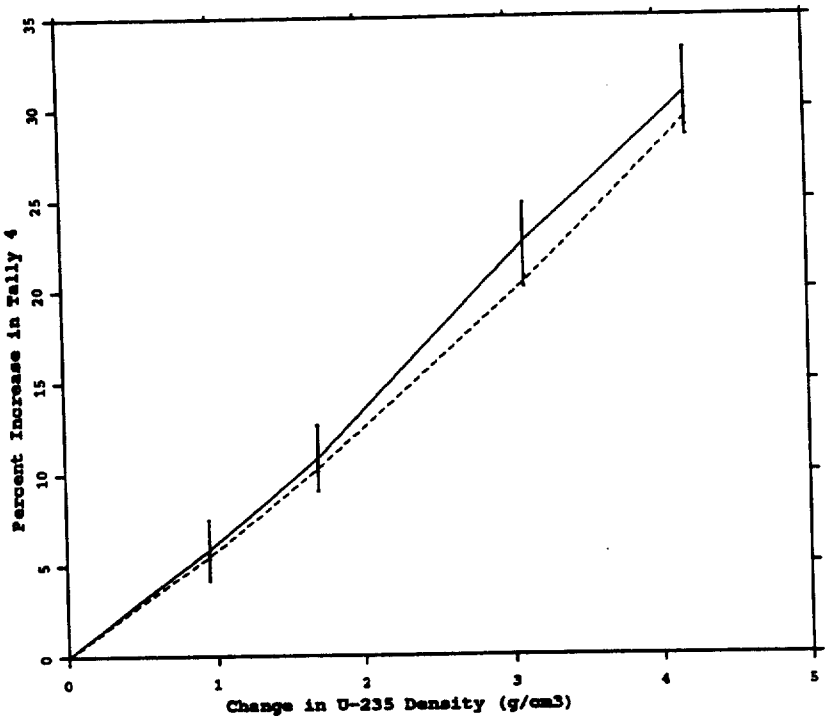

Fig. 17. Change in Tally 4 of problem INP11 due to an increase in the ^{235}U density. Solid line is Actual and dashed line is Predicted.

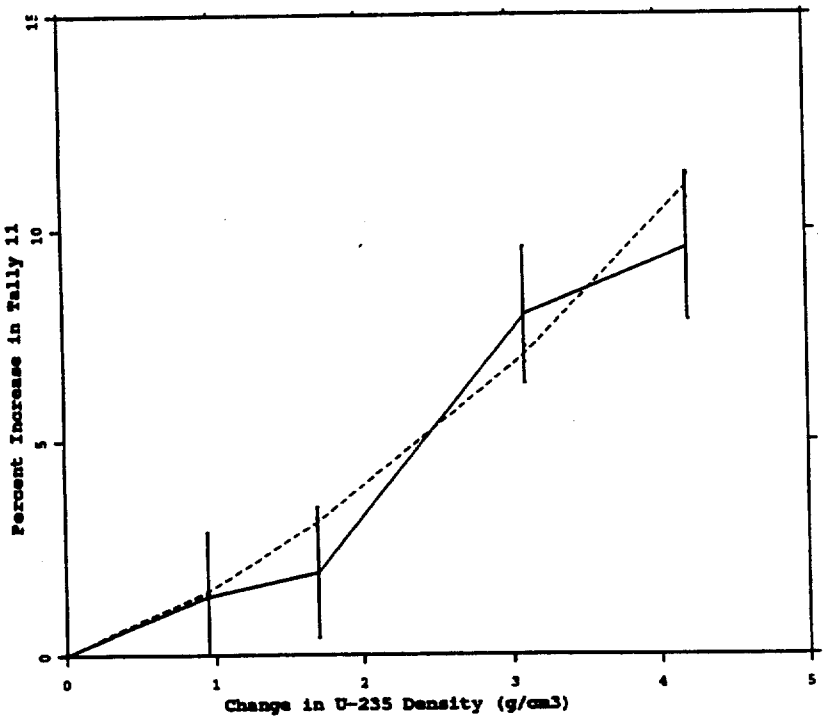

Fig. 18. Change in Tally 11 of problem INP11 due to an increase in the ^{235}U density. Solid line is Actual and dashed line is Predicted.

D. Criticality Problems

Two criticality problems were chosen for inclusion in this report. The following sections include a short description of the geometry followed by a discussion of the actual and predicted perturbation results.

1. Test Problem INP09. Input file INP09 consists of a 10 cm cube filled with ^{235}U (see Fig. 19). Two rectangular pieces of copper are implanted in this cube, and a cone-shaped hole extends from one side into the center. A second cone-shaped region of ^{235}U protrudes from another side of the cube. The cube is surrounded by a sphere of air (20 cm radius). This problem was executed in criticality mode and had a final combined k_{eff} of 1.0133 ± .00015.

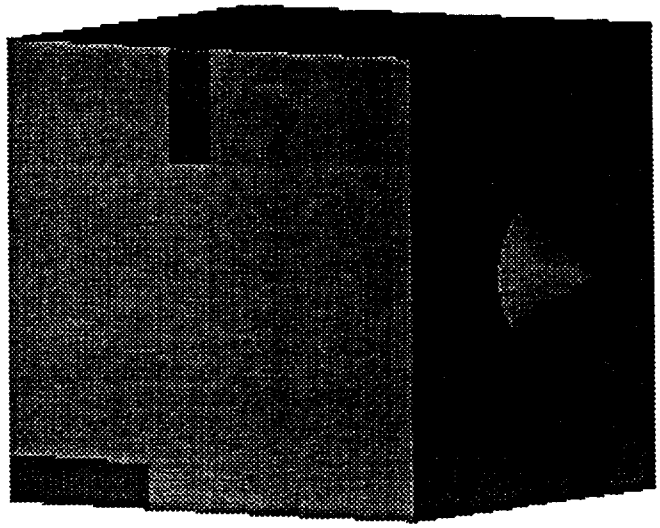

Fig. 19. Geometry plot of test problem INP09.

Tally 14, a track-length estimate of k_{eff}, was added to this problem to estimate the effect of the perturbation on the eigenvalue. The surrounding air density was increased from 0.01 g/cm^3 to 0.49, 0.90, 2.0, and 3.0 g/cm^3. Table XI gives the corresponding increase in Tally 14 of 5.13%, 9.62%, 20.35%, and 29.13% for the actual change and 6.69%, 12.31%, 27.01%, and 39.87% for the predicted change. Figure 20 plots these results as a function of the differential increase in air density. Clearly the predicted increase in k_{eff} is overestimated by a few percent. This overestimation is probably due to the fact that the differential operator technique does not currently account for changes in the shape of the eigenfunction that result from a perturbation.

TABLE XI
ACTUAL AND PREDICTED PERTURBATION RESULTS FOR TALLY 14 OF PROBLEM INP09

	Air Density (g/cm^3)=	0.01	0.49	0.90	2.00	3.00
Actual	k_{eff}	1.0095	1.0613	1.1066	1.2149	1.3036
	Relative Error	0.0001	0.0014	0.0014	0.0015	0.0015
	% Change		5.13%	9.62%	20.35%	29.13%
	Relative Error		0.0288	0.0160	0.0089	0.0067
Predicted	Change in k_{eff}		6.7537E-2	0.1243	0.2727	0.4025
	Relative Error		0.0197	0.0355	0.0797	0.1216
	% Change		6.69%	12.31%	27.01%	39.87%
	Relative Error		0.0197	0.0355	0.0797	0.1216

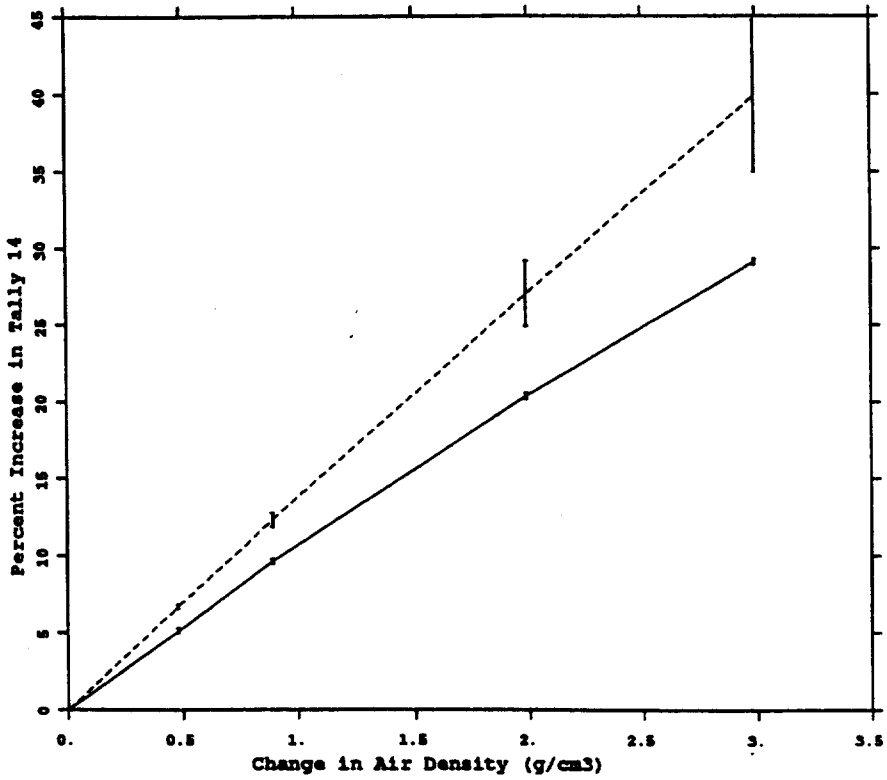

Fig. 20. Change in Tally 14 of problem INP09 due to an increase in the air density. Solid line is Actual and dashed line is Predicted.

2. **Test Problem INP18.** Input file INP18 includes a triangular pitched nuclear reactor core. The hexagonal lattice of fuel rods is contained within a cylindrical core. Five whole and three partial control rods, filled with a mixture of boron and carbon, are included in the core. The fuel rods are 70% enriched uranium (labeled as region "2" in Fig. 21), and the clad on the fuel is a mixture of zirconium and niobium with a inner liner of tungsten. Inside the clad, the fuel is cooled by a water blanket. Water is also used as the moderator and heat transfer agent between the fuel rods. The water is a mixture of heavy and light water. When executed in criticality mode, this problem produced a final combined k_{eff} of 1.0379 ± .0002.

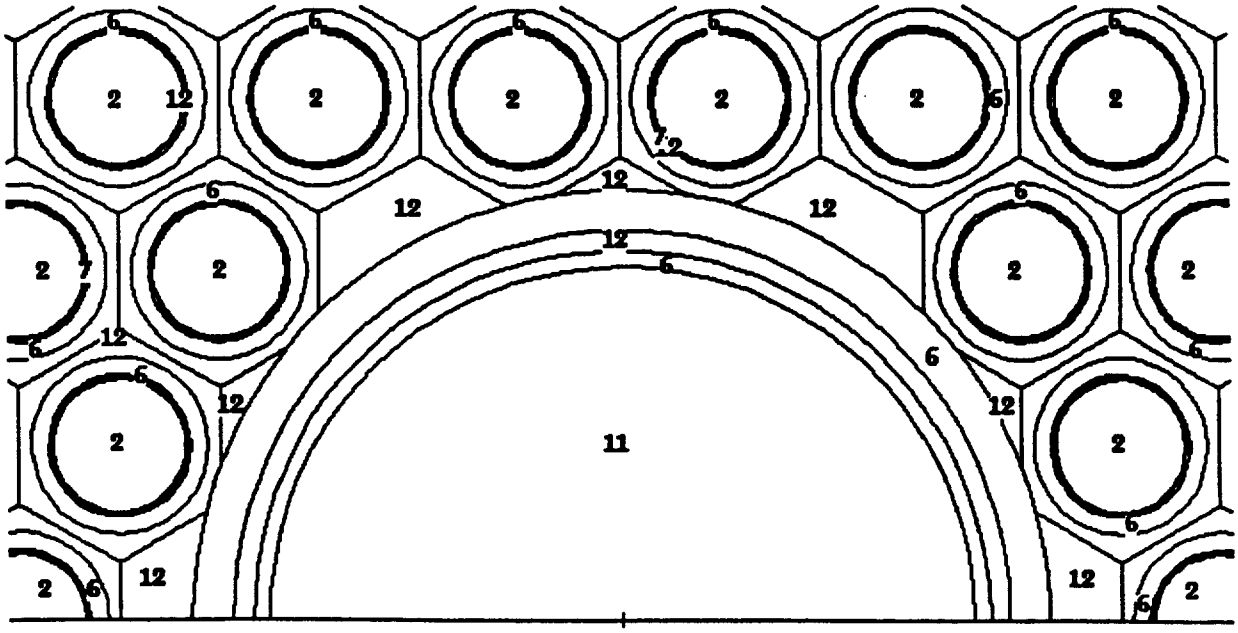

Fig. 21. Geometry plot of test problem INP18.

Again Tally 14 was added to this input file to produce a track-length estimate of k_{eff}. The water density was increased from 1.0 g/cm^3 to 1.5, 2.3, 4.0, and 6.0 g/cm^3. Table XII gives the corresponding increase in Tally 14 of 4.49%, 10.46%, 20.80%, and 30.02% for the actual change and 4.83%, 11.00%, 19.68%, and 21.60% for the predicted change. Figure 22 plots these results as a function of the differential increase in water density. These curves show good agreement within the reported one-sigma statistical uncertainties up to the 20% data point.

TABLE XII
ACTUAL AND PREDICTED PERTURBATION RESULTS FOR TALLY 14 OF PROBLEM INP18

	Water Density (g/cm^3)=	1.0	1.5	2.3	4.0	6.0
Actual	k_{eff}	1.0371	1.0837	1.1456	1.2528	1.3484
	Relative Error	0.0003	0.0016	0.0018	0.0020	0.0021
	% Change		4.49%	10.46%	20.80%	30.02%
	Relative Error		0.0378	0.0192	0.0117	0.0092
Predicted	Change in k_{eff}		5.0076E-2	0.1141	0.2041	0.2240
	Relative Error		0.0097	0.0168	0.0429	0.1053
	% Change		4.83%	11.00%	19.68%	21.60%
	Relative Error		0.0097	0.0168	0.0429	0.1053

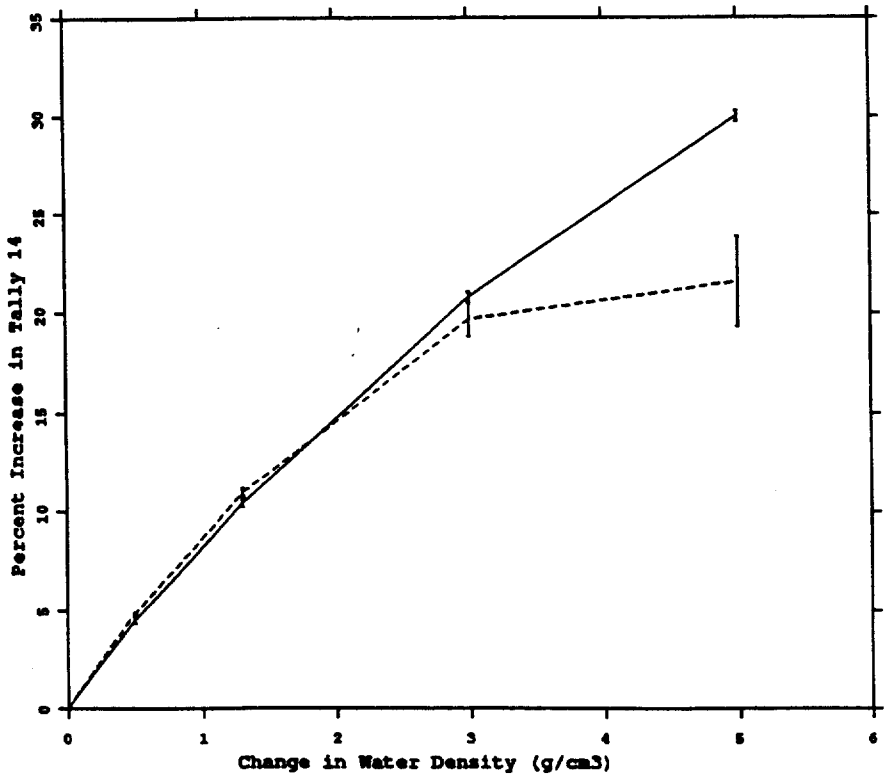

Fig. 22. Change in Tally 14 of problem INP18 due to an increase in the water density. Solid line is Actual and dashed line is Predicted.

E. First Order Versus Second Order

This section discusses the relevance and range of applicability of the first and second order terms of the Taylor series expansion (see Section II.A.). Clearly, if a response is a linear function of a perturbed parameter, the first order estimator will accurately predict any size of change in that response — likewise for a response that exhibits a quadratic behavior and a second order estimator is added. However, as demonstrated in the previous test problems, this rarely occurs over the range of interest. Figure 23 presents the perturbation results for test problem INP02 with the first order estimator separated from the default (first plus second order) estimator. In this case, the second order term clearly makes a significant contribution to predicted changes in the response that exceed 10%.

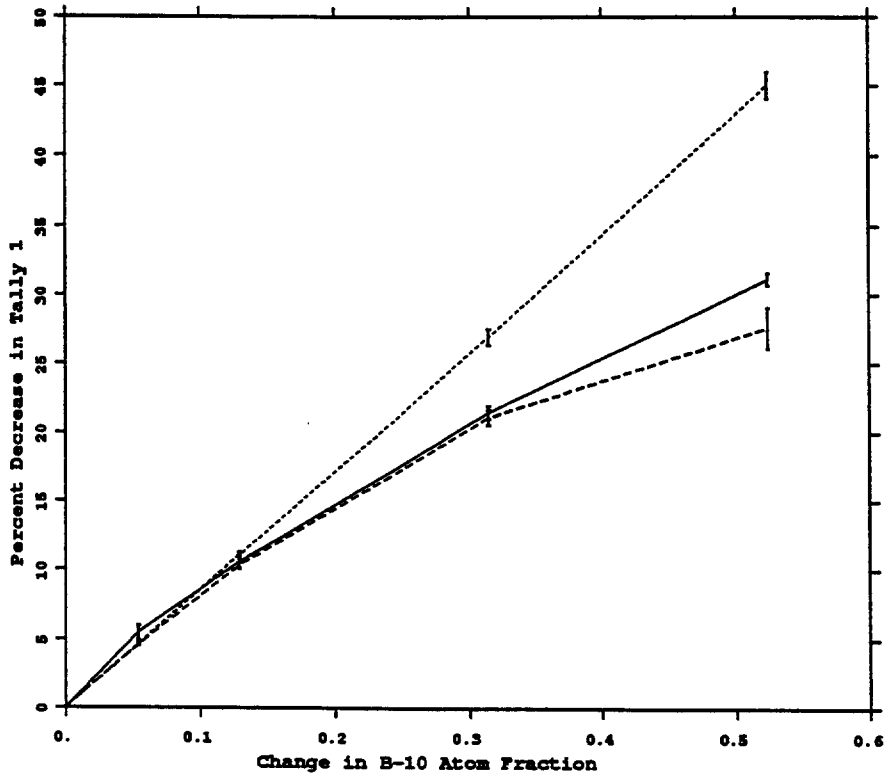

Fig. 23. Change in Tally 1 of problem INP02 due to an increase in the ^{10}B atom fraction. Solid line gives the actual change; dashed line gives the first and second order predicted change; dotted line gives the first order predicted change.

Analyzing the first and second order results of the previous test problems leads to the following rules of thumb. The first order perturbation estimator typically provides sufficient accuracy for response changes that are less than 5%. The default first and second order estimator offers acceptable accuracy for response changes that are less than 20%-30%. This upper bound depends on the behavior of the response as a function of the perturbed parameter. The magnitude of the second order estimator is a good measure of the range of applicability. If this magnitude exceeds 30% of the first order estimator, it is likely that higher order terms are needed for an accurate prediction. The METHOD keyword on the PERT card (see Section III) allows one to tally the second order term separate from the first. The following PERT cards demonstrate this:

```
PERT1:n cell=1 rho=-3.5
PERT2:n cell=1 rho=-3.5 method=2
PERT3:n cell=1 rho=-3.5 method=3
```

The first PERT card generates the default (first plus second order) perturbation results; the second produces only first order results; and the third gives only second order results. Once the behavior of a perturbation is understood, unneeded PERT cards can be removed from future analyses.

V. SUMMARY

Results presented in this report verify the applicability of the differential operator perturbation technique as implemented within MCNP. This capability is shown to be relevant for fixed-source problems (neutron, photon, and coupled neutron/photon) as well as criticality applications. Furthermore, this technique can be used to estimate the effects of multiple perturbations in a single run with minimal loss (5%-10% per perturbation) of performance. A key advantage of this method is that the precision of the estimator remains bounded, even as the magnitude of the perturbation vanishes.

Table XIII summarizes the perturbation results presented in this report. In general, the accuracy of the differential operator technique appears to be within a couple percent for up to 20%-30% changes in a response. Exceptions to this include test problems INP09 and INP10. The most likely explanation for the deviation of test problem INP09 is that this technique does not currently account for perturbations in the shape of the eigenfunction. The deviation shown for the photon tally of test problem INP10 is due to the higher order behavior of the response perturbation which cannot be estimated accurately by first and second order terms of the Taylor series expansion (see

Fig. 15). For small response perturbations (< 5%), it was found that use of only the first order estimator typically offers sufficient accuracy.

Possible enhancements to the MCNP perturbation feature include compatibility with point detectors, DXTRAN spheres, k_{eff} estimators, and electron transport. While application of the differential operator technique to the first three areas is fairly straightforward,[17,18] its application to electron transport has not yet been investigated. Future effort related to the perturbation feature will also include additional verification work, with an emphasis on experimental applications.

TABLE XIII
SUMMARY OF MCNP PERTURBATION RESULTS

Test Problem	First Perturbation ~5%			Second Perturbation ~10%			Third Perturbation ~20%			Fourth Perturbation ~30%		
	Actual	PERT	Diff	Actual	PERT	Diff	Actual	PERT	Diff	Actual	PERT	Diff
Neutron Fixed-Source												
INP01	5.02% (.0695)	4.75% (.0061)	-0.27%	10.38% (.0341)	10.28% (.0064)	-0.10%	20.36% (.0176)	20.59% (.0071)	0.23%	28.58% (.0129)	28.65% (.0076)	0.07%
INP02	-5.47% (.0924)	-4.59% (.0193)	-0.88%	-10.56% (.0469)	-10.32% (.0189)	-0.24%	-21.46% (.0221)	-21.11% (.0268)	-0.35%	-31.15% (.0146)	-27.65% (.0532)	-3.50%
INP07	5.27% (.1887)	5.83% (.0351)	0.56%	9.77% (.1102)	9.31% (.0365)	-0.46%	20.62% (.0556)	19.47% (.0402)	-1.15%	33.98% (.0381)	31.52% (.0443)	-2.46%
INP12	5.88% (.1924)	3.54% (.0088)	-2.34%	10.45% (.1103)	9.97% (.0090)	-0.48%	20.91% (.0586)	18.91% (.0093)	-2.00%	30.19% (.0418)	29.24% (.0095)	-0.95%
INP14	4.46% (.2840)	3.50% (.0117)	-0.96%	10.54% (.1293)	8.63% (.0191)	-1.91%	20.30% (.0712)	23.16% (.0380)	2.86%	30.13% (.0523)	46.45% (.0608)	16.32%
Photon Fixed-Source												
INP04	-4.69% (.0635)	-4.73% (.0158)	0.04%	-9.17% (.0331)	-9.30% (.0144)	0.13%	-18.52% (.0168)	-19.09% (.0128)	0.57%	-23.62% (.0135)	-24.75% (.0134)	1.13%
Coupled Neutron/Photon Fixed-Source												
INP10 Neutron	4.82% (.2094)	3.99% (.0268)	-0.83%	7.80% (.1288)	7.79% (.0305)	-0.01%	20.43% (.0522)	20.45% (.0496)	0.02%	28.09% (.0385)	29.51% (.0666)	1.42%
INP10 Photon	5.82% (.1606)	6.04% (.0217)	0.22%	11.51% (.0833)	12.13% (.0244)	0.62%	28.10% (.0357)	34.97% (.0381)	6.87%	4.41% (.1939)	53.84% (.0488)	49.43%
INP11 Neutron	5.82% (.2900)	5.45% (.0120)	-0.37%	10.83% (.1651)	10.25% (.0126)	-0.58%	22.68% (.0925)	20.40% (.0140)	-2.28%	30.81% (.0764)	29.44% (.0151)	-2.37%
INP11 Photon	1.37% (1.0989)	1.49% (.0313)	0.12%	1.92% (.7944)	3.09% (.0290)	1.17%	7.97% (.2047)	7.03% (.0273)	-0.94%	9.56% (.1778)	11.02% (.0269)	1.46%
Criticality												
INP09	5.13% (.0288)	6.69% (.0197)	1.56%	9.62% (.0160)	12.31% (.0355)	2.69%	20.35% (.0089)	27.01% (.0797)	6.66%	29.13% (.0067)	39.87% (.1216)	10.74%
INP18	4.49% (.0378)	4.83% (.0097)	0.34%	10.46% (.0192)	11.00% (.0168)	0.54%	20.80% (.0117)	19.68% (.0429)	-1.12%	30.02% (.0092)	21.60% (.1053)	-8.42%

REFERENCES

1. J. Briesmeister, Editor, "MCNP — A General Monte Carlo N-Particle Transport Code," LA-12625-M, Los Alamos National Laboratory (1993).

2. J. E. Olhoeft, "The Doppler Effect for a Non-Uniform Temperature Distribution in Reactor Fuel Elements," WCAP-2048, Westinghouse Electric Corporation, Atomic Power Division, Pittsburgh (1962).

3. H. Takahashi, "Monte Carlo Method for Geometrical Perturbation and its Application to the Pulsed Fast Reactor," Nucl. Sci. Eng. **41**, p. 259 (1970).

4. M. C. Hall, "Monte Carlo Perturbation Theory in Neutron Transport Calculations," Ph. D. Thesis, University of London (1980).

5. M. C. Hall, "Cross-Section Adjustment with Monte Carlo Sensitivities: Application to the Winfrith Iron Benchmark," Nucl. Sci. Eng. **81**, p. 423 (1982).

6. H. Rief, "Generalized Monte Carlo Perturbation Algorithms for Correlated Sampling and a Second-Order Taylor Series Approach," Ann. Nucl. Energy **11**, p. 455 (1984).

7. G. McKinney, "A Monte Carlo (MCNP) Sensitivity Code Development and Application," M.S. Thesis, University of Washington (1984).

8. W. Matthes, "Monte Carlo Calculation of the Nuclear Temperature Coefficient in Fast Reactors," Proc. 3rd Symp. "Reactor Theory" of EURATOM, EUR-309.e (1963).

9. M. E. Gubbins, "Reactor Perturbation Calculations by Monte Carlo Methods," United Kingdom Atomic Energy Authority, AEEW-M-581 (1966).

10. T. J. Hoffman and L. M. Petrie, "Monte Carlo Reactivity Calculations Using a Perturbation Source," Trans. Am. Nucl. Soc., **15**, p. 912 (1972).

11. W. Matthes, "Calculation of Reactivity Perturbations with the Monte Carlo Method," Nucl. Sci. Eng., **47**, p. 234 (1972).

12. H. Kschwendt and H. Rief, "TIMOC: A General Purpose Monte Carlo Code for Stationary and Time Dependent Neutron Transport," EUR-4519 (1970).

13. W. Bernnat, "Monte Carlo Technique for Local Perturbations in Multiplying Systems," Proc. NEACRP Specialist Meeting, ANL-75-2, p. 261 (1974).

14. M. Nakagawa and T. Asaoka, "Improvement of Correlated Sampling Monte Carlo Methods for Reactivity Calculations," Nucl. Sci. Tech., **15**, p. 400 (1978).

15. W. E. Preeg and J. S. K.Tsang, "Comparison of Correlated Monte Carlo Techniques," Trans. Am. Nucl. Soc., 43, p. 628 (1982).

16. G. W. McKinney, "Theory Related to the Differential Operator Perturbation Technique," Los Alamos National Laboratory Memo, X-6:GWM-94-124 (1994).

17. R. L. Perel et al., "Monte Carlo Calculation of Point Detector Sensitivities to Cross Sections," Proceedings of the International Conference on Mathematics and Computations - Reactor Physics and Environmental Analyses, April 30-May 4, Portland, Oregon, p. 1479 (1995).

18. F. X. Gallmeier, "A New MCNP Option: KCORR — The Use of the Correlated Sampling Method to Study Reactivity Effects Due to Changes of a Reactor Arrangement," Nucl. Sci. Eng., 120, p. 102 (1995).

APPENDIX A

MCNP INPUT FILES

I. OVERVIEW

The MCNP input files used to generate the "predicted" perturbation results are included in this appendix. These input files are nearly identical to those provided with the MCNP 4A distribution package. Lines that have been added or modified relative to the distribution test set appear in bold type below. These lines include the material and PERT cards needed to invoke the perturbation analysis as well as modifications to disable unnecessary or incompatible features. The MCNP input files used to generate the "actual" perturbation results are not included in this appendix, due to their voluminous redundancy. Again these input files are nearly identical to those in the distribution set except for the slight modifications needed to implement the perturbation specified on the related PERT card. For example, the four input files generated for test problem INP01 involved modifying one number in the input file (i.e., changing the density for cell 1 to 1.85, 1.40, 0.6, and 0.005 g/cm^3).

A. Neutron Fixed-Source Problems

1. Test Problem INP01.

```
prob1 -- simple neutron problem to test some basic operations of mcnp.
1     1  -2.25    -1  imp:n=1   $ graphite ball
2     2  -8.95  1 -2  imp:n=1   $ copper shell
3     0         2 -3  imp:n=1   $ void space
4     0         3     imp:n=0   $ zero-importance outside world

1     so  5
2     so  7.5
3     so 10

c    biased isotropic point source at (0,0,0)
sdef  erg d1   vec 0 1 0   dir d2   tme d5
sc5  equiprobable bin treatment for time distribution.
si5  -50 -10 3i 10 5m
sp5  -41 10
sb5  0 .1 .2 .3 1r .2 .1
sc1  flat energy spectrum from 1 to 14.1 mev.
si1   1 14.1
sp1   0 1
sc2  direction is biased toward the point detector.
sb2   -31 1.5
c
m2    29000.40 1
m1     6012.40c 1
```

```
awtab 6012. 11.8969
c    xs3  6012.50c 11.8969 rmccs 0 3 92853 23390 0 0 2.53e-08
phys:n  14.2 .01
c
fc1  current across the graphite-copper interface.
f1:n  1
e1    .1 .5 .8 2 4 12 14.1
c1    -.866 -.5 0 .5 .866 1
em1  1 5i 7
cm1  8 4i 13
tm5  14 8i 23
t5   -50 -10 3i 10 5m 4m 5m 1.e20
fq1   c e
fc5  flux at a point in the void just outside the copper shell.
f5:n  0 8 0 0
e5    .1 .5 .8 2 4 12 14.1
c
pert1:n cell=1 rho=-1.850
pert2:n cell=1 rho=-1.400
pert3:n cell=1 rho=-0.600
pert4:n cell=1 rho=-0.005
cut:n 1.e20 .05 .05 .01 .01
nps   1000000
print -98
prdmp 2j -1
dbcn j 1000 512 513 2j 100 10000 5 $ non-multitask version.
c    dbcn 6j 100 10000 5 $ dbcn card for multitask version.
```

2. Test Problem INP02.

```
prob2 -- three different tallies of the same physical quantity
1     1  -2.45    -1     $ boron ball with volume source
2     2  -2.7   1 -2 4   $ aluminum shell
3     2  -2.7   2 -3 4   $ aluminum shell
4     0         3        $ outside world
5     2  -2.7   5 -4     $ big aluminum ball to avoid dxtran/tally2 conflict
6     2  -2.7     -5     $ little aluminum ball for tally 4

1     so  5
2     so  7
3     so 10
4     sy  7   1.95
5     sy  7    .3

c    volume source in boron ball, biased in position.
c    the symmetry is sufficient for the bias to be a fair game.
sdef  cel 1   x d1   y d2   z d3   erg d4
si1   -5 5
sp1    0 1
sc2  position is biased toward the dxtran and the ring detector.
si2   a -5 5
sp2   1 1
sb2   1 2
si3   -5 5
sp3    0 1
sc4  flat energy spectrum from .1 to 1 mev.
si4   .1 1
sp4    0 1
```

```
c
m1      5010.03d .196 5011.40c .804    $ natural boron
m2     13027.40c 1    $ aluminum-27
m3      5010.03d .250 5011.40c .750    $ enriched b-10 of .250
m4      5010.03d .325 5011.40c .675    $ enriched b-10 of .325
m5      5010.03d .510 5011.40c .490    $ enriched b-10 of .510
m6      5010.03d .720 5011.40c .280    $ enriched b-10 of .720
pert1:n  cell=1  mat=3
pert2:n  cell=1  mat=4
pert3:n  cell=1  mat=5
pert4:n  cell=1  mat=6
ctme 60
phys:n  1.2      $ cross sections above 1.2 mev will be expunged.
c
c    all tallies have the same energy bins.
e0     .01 .03 .1 .3 1
fc2  average flux on surface 2.
f2:n  2
f1:n 1
c1    -.8 8i 1 t
fq1   c e
tf1   1 7r
ft2   tmc -2 .05
t2    -2 9i 3 10 100
fq2   t e
ft1   frv 3 4 5    geb 1 2 0
fc4   average flux in cell 6.
f4:n  6
pd5   .3 1 4r
dd5   .003
fq5   u e
fu5   1 8i 10
ft5   inc
fc5   average flux at ring detector.
fy5:n 5 4.89 .7
c      dxc:n  1 .7 .9 0 1 1
c      dd1   .04 100
thtme -10 0 .5 1 2
#     tmp1   tmp2   tmp3   tmp4   tmp5
   1  1e-8   2e-8   3e-8   4e-8   5e-8
   2  2e-8   3e-8   5e-8   4e-8   3e-8
   3  1e-8   5e-8   4e-8   3e-8   2e-8
   4     0      0      0      0      0
   5  2e-8   1e-8   5e-8   3e-8   1e-8
   6  3e-8   2e-8   1e-8   2e-8   1e-8
c
c      dxt:n 0 7 0 1 1.9  $ dxtran around cell 6, inside cell 5.
imp:n 1 1 1 0 1 1
c
cut:n j .001        $ energy cutoff at .001 mev.
nps   100000          $ run 5000 histories.
print -98           $ print all possible output for easier debugging.
prdmp 2j -1         $ print mctal file.
ptrac buffer=2 file=asc event=src nps=1,200 cell=3
```

3. Test Problem INP07.

```
prob7 -- generate surface source for prob8
1     0   12                  $ zero-importance outside world
2     0   -12 (7:1:-2)        $ empty space
3     5 -5.2   -7 -1 2 #4 #5  $ rusty box
4     6 -8.1   -5 -4 3        $ source cell:  uranium oxide
5     7 -2.7   -7 -6 5        $ aluminum stuffer

1     cx 15
2     px 0
3     px 10
4     cx 5
5     px 20
6     c/x 2.5 0 2.5
7     px 40
12    so 170

m5    26000.40c 1  8016.40c 1
m6    92235.40c 1  8016.40c 2
m7    13027.40c 1
pert1:n cell=4 rho=-8.8
pert2:n cell=4 rho=-9.2
pert3:n cell=4 rho=-10.3
pert4:n cell=4 rho=-11.5
drxs
imp:n  0 0 1 2r
ssw   7      $ write the surface source at surface 7
c
sdef  erg d1   cel 4   axs 1 0 0   rad d3   ext d2   vec 1 0 0   dir d5
si1   a 1 2 4 7
sp1   0 2 1 0
sc2   the symmetry makes it a fair game.
si2   10 12 14 16 18 20
sp2   0 1 4r
sb2   0 1 2 3 4 5
si3   0 5
sp3   -21 1
si5   -1 -.5 0 .5 1
sp5   0 1 3r
sb5   0 1 2 3 4
c
f2:n  7
e0    .1 .5 1 2 10
f7:n   4
sd2   706.858    $ area of surface 7
cut:n  j .01
nps   100000
prdmp 2j -1
print -98
```

4. Test Problem INP12.

```
prob12  ==>> porosity tool model
c    ============================================================
c    ============================================================
c    ===>>>  run        : prob12
c    ===>>>  tool       : generic porosity tool
c    ===>>>  source     : ambe
```

```
c    ===>>>  borehole  : 8" bh, fw
c    ===>>>  formation : 20 pu limestone, fw
c    ===>>>  casing    : none
c    ===>>>  detector  : he-3 at 4 atomospheres
c    ===>>>              near : 1"odx3"  at 7.5" centerline from source
c    ===>>>              far  : 2"odx10" at  20" centerline from source
c    ===>>>  shielding : none
c    ===>>>  sonde     : solid iron
c    ===>>>  weights   : xtrapt/diffusion
c    ===>>>   generate weights using wep patch with factor of 2.0 to far det
c    ===>>>       using a factor of 8.0; only use 50k particles
c    ===>>>  physics   : thermal cutin changed to -200
c    ===>>>              s(a,b) added for water
c    ============================================================
c    ============================================================
c
c
c    ============================================================
c    ===== zone cards
c    ============================================================
c    ===== near detector
c    ============================================================
c
   1    1   -0.000502     -1     +13     -14                      $ det_n
c
c    ============================================================
c    ===== far detector
c    ============================================================
c
   2    1   -0.000502     -2     +16     -19                      $ det_f
c
c    ============================================================
c    ===== source region
c    ============================================================
c
   3    2   -7.86         -3     +11     -12                      $ sourc
c
c    ============================================================
c    ===== iron sonde
c    ============================================================
c
   4    2   -7.86         -3     +10     -11                      $ sonde
   5    2   -7.86         -3     +12     -13                      $ sonde
   6    2   -7.86         +1      -3     +13     -14              $ sonde
   7    2   -7.86         -3     +14     -15                      $ sonde
   8    2   -7.86         -3     +15     -16                      $ sonde
   9    2   -7.86         +2      -3     +16     -17              $ sonde
  10    2   -7.86         +2      -3     +17     -18              $ sonde
  11    2   -7.86         +2      -3     +18     -19              $ sonde
  12    2   -7.86         -3     +19     -20                      $ sonde
  13    2   -7.86         -3     +20     -21                      $ sonde
  14    2   -7.86         -3     +21     -22                      $ sonde
c
c    ============================================================
c    ===== borehole
c    ============================================================
c
  15    3   -1.0          +3      -5      -4     +10     -11       $ bh
  16    3   -1.0          +3      -5      -4     +11     -12       $ bh
```

```
 17    3   -1.0          +3      -5      -4      +12     -13             $ bh
 18    3   -1.0          +3      -5      -4      +13     -14             $ bh
 19    3   -1.0          +3      -5      -4      +14     -15             $ bh
 20    3   -1.0          +3      -5      -4      +15     -16             $ bh
 21    3   -1.0          +3      -5      -4      +16     -17             $ bh
 22    3   -1.0          +3      -5      -4      +17     -18             $ bh
 23    3   -1.0          +3      -5      -4      +18     -19             $ bh
 24    3   -1.0          +3      -5      -4      +19     -20             $ bh
 25    3   -1.0          +3      -5      -4      +20     -21             $ bh
 26    3   -1.0          +3      -5      -4      +21     -22             $ bh
 27    3   -1.0          +3      -5      +4      +10     -11             $ bh
 28    3   -1.0          +3      -5      +4      +11     -12             $ bh
 29    3   -1.0          +3      -5      +4      +12     -13             $ bh
 30    3   -1.0          +3      -5      +4      +13     -14             $ bh
 31    3   -1.0          +3      -5      +4      +14     -15             $ bh
 32    3   -1.0          +3      -5      +4      +15     -16             $ bh
 33    3   -1.0          +3      -5      +4      +16     -17             $ bh
 34    3   -1.0          +3      -5      +4      +17     -18             $ bh
 35    3   -1.0          +3      -5      +4      +18     -19             $ bh
 36    3   -1.0          +3      -5      +4      +19     -20             $ bh
 37    3   -1.0          +3      -5      +4      +20     -21             $ bh
 38    3   -1.0          +3      -5      +4      +21     -22             $ bh
c
c    ================================================================
c    ===== formation region to radius=15 cm
c    ================================================================
c
 39    4   -2.3688       +5      -6      -23     -24     +10     -11     $ form
 40    4   -2.3688       +5      -6      -23     -24     +11     -12     $ form
 41    4   -2.3688       +5      -6      -23     -24     +12     -13     $ form
 42    4   -2.3688       +5      -6      -23     -24     +13     -14     $ form
 43    4   -2.3688       +5      -6      -23     -24     +14     -15     $ form
 44    4   -2.3688       +5      -6      -23     -24     +15     -16     $ form
 45    4   -2.3688       +5      -6      -23     -24     +16     -17     $ form
 46    4   -2.3688       +5      -6      -23     -24     +17     -18     $ form
 47    4   -2.3688       +5      -6      -23     -24     +18     -19     $ form
 48    4   -2.3688       +5      -6      -23     -24     +19     -20     $ form
 49    4   -2.3688       +5      -6      -23     -24     +20     -21     $ form
 50    4   -2.3688       +5      -6      -23     -24     +21     -22     $ form
 51    4   -2.3688       +5      -6      -23     +24     +10     -11     $ form
 52    4   -2.3688       +5      -6      -23     +24     +11     -12     $ form
 53    4   -2.3688       +5      -6      -23     +24     +12     -13     $ form
 54    4   -2.3688       +5      -6      -23     +24     +13     -14     $ form
 55    4   -2.3688       +5      -6      -23     +24     +14     -15     $ form
 56    4   -2.3688       +5      -6      -23     +24     +15     -16     $ form
 57    4   -2.3688       +5      -6      -23     +24     +16     -17     $ form
 58    4   -2.3688       +5      -6      -23     +24     +17     -18     $ form
 59    4   -2.3688       +5      -6      -23     +24     +18     -19     $ form
 60    4   -2.3688       +5      -6      -23     +24     +19     -20     $ form
 61    4   -2.3688       +5      -6      -23     +24     +20     -21     $ form
 62    4   -2.3688       +5      -6      -23     +24     +21     -22     $ form
 63    4   -2.3688       +5      -6      +23     -24     +10     -11     $ form
 64    4   -2.3688       +5      -6      +23     -24     +11     -12     $ form
 65    4   -2.3688       +5      -6      +23     -24     +12     -13     $ form
 66    4   -2.3688       +5      -6      +23     -24     +13     -14     $ form
 67    4   -2.3688       +5      -6      +23     -24     +14     -15     $ form
 68    4   -2.3688       +5      -6      +23     -24     +15     -16     $ form
 69    4   -2.3688       +5      -6      +23     -24     +16     -17     $ form
 70    4   -2.3688       +5      -6      +23     -24     +17     -18     $ form
```

```
 71    4   -2.3688        +5      -6      +23     -24     +18     -19     $ form
 72    4   -2.3688        +5      -6      +23     -24     +19     -20     $ form
 73    4   -2.3688        +5      -6      +23     -24     +20     -21     $ form
 74    4   -2.3688        +5      -6      +23     -24     +21     -22     $ form
 75    4   -2.3688        +5      -6      +23     +24     +10     -11     $ form
 76    4   -2.3688        +5      -6      +23     +24     +11     -12     $ form
 77    4   -2.3688        +5      -6      +23     +24     +12     -13     $ form
 78    4   -2.3688        +5      -6      +23     +24     +13     -14     $ form
 79    4   -2.3688        +5      -6      +23     +24     +14     -15     $ form
 80    4   -2.3688        +5      -6      +23     +24     +15     -16     $ form
 81    4   -2.3688        +5      -6      +23     +24     +16     -17     $ form
 82    4   -2.3688        +5      -6      +23     +24     +17     -18     $ form
 83    4   -2.3688        +5      -6      +23     +24     +18     -19     $ form
 84    4   -2.3688        +5      -6      +23     +24     +19     -20     $ form
 85    4   -2.3688        +5      -6      +23     +24     +20     -21     $ form
 86    4   -2.3688        +5      -6      +23     +24     +21     -22     $ form
c
c    ================================================================
c    ===== formation region to radius=25 cm
c    ================================================================
c
 87    4   -2.3688        +6      -7      -23     -24     +10     -11     $ form
 88    4   -2.3688        +6      -7      -23     -24     +11     -12     $ form
 89    4   -2.3688        +6      -7      -23     -24     +12     -13     $ form
 90    4   -2.3688        +6      -7      -23     -24     +13     -14     $ form
 91    4   -2.3688        +6      -7      -23     -24     +14     -15     $ form
 92    4   -2.3688        +6      -7      -23     -24     +15     -16     $ form
 93    4   -2.3688        +6      -7      -23     -24     +16     -17     $ form
 94    4   -2.3688        +6      -7      -23     -24     +17     -18     $ form
 95    4   -2.3688        +6      -7      -23     -24     +18     -19     $ form
 96    4   -2.3688        +6      -7      -23     -24     +19     -20     $ form
 97    4   -2.3688        +6      -7      -23     -24     +20     -21     $ form
 98    4   -2.3688        +6      -7      -23     -24     +21     -22     $ form
 99    4   -2.3688        +6      -7      -23     +24     +10     -11     $ form
100    4   -2.3688        +6      -7      -23     +24     +11     -12     $ form
101    4   -2.3688        +6      -7      -23     +24     +12     -13     $ form
102    4   -2.3688        +6      -7      -23     +24     +13     -14     $ form
103    4   -2.3688        +6      -7      -23     +24     +14     -15     $ form
104    4   -2.3688        +6      -7      -23     +24     +15     -16     $ form
105    4   -2.3688        +6      -7      -23     +24     +16     -17     $ form
106    4   -2.3688        +6      -7      -23     +24     +17     -18     $ form
107    4   -2.3688        +6      -7      -23     +24     +18     -19     $ form
108    4   -2.3688        +6      -7      -23     +24     +19     -20     $ form
109    4   -2.3688        +6      -7      -23     +24     +20     -21     $ form
110    4   -2.3688        +6      -7      -23     +24     +21     -22     $ form
111    4   -2.3688        +6      -7      +23     -24     +10     -11     $ form
112    4   -2.3688        +6      -7      +23     -24     +11     -12     $ form
113    4   -2.3688        +6      -7      +23     -24     +12     -13     $ form
114    4   -2.3688        +6      -7      +23     -24     +13     -14     $ form
115    4   -2.3688        +6      -7      +23     -24     +14     -15     $ form
116    4   -2.3688        +6      -7      +23     -24     +15     -16     $ form
117    4   -2.3688        +6      -7      +23     -24     +16     -17     $ form
118    4   -2.3688        +6      -7      +23     -24     +17     -18     $ form
119    4   -2.3688        +6      -7      +23     -24     +18     -19     $ form
120    4   -2.3688        +6      -7      +23     -24     +19     -20     $ form
121    4   -2.3688        +6      -7      +23     -24     +20     -21     $ form
122    4   -2.3688        +6      -7      +23     -24     +21     -22     $ form
123    4   -2.3688        +6      -7      +23     +24     +10     -11     $ form
124    4   -2.3688        +6      -7      +23     +24     +11     -12     $ form
```

```
 125    4   -2.3688        +6      -7      +23     +24     +12     -13     $ form
 126    4   -2.3688        +6      -7      +23     +24     +13     -14     $ form
 127    4   -2.3688        +6      -7      +23     +24     +14     -15     $ form
 128    4   -2.3688        +6      -7      +23     +24     +15     -16     $ form
 129    4   -2.3688        +6      -7      +23     +24     +16     -17     $ form
 130    4   -2.3688        +6      -7      +23     +24     +17     -18     $ form
 131    4   -2.3688        +6      -7      +23     +24     +18     -19     $ form
 132    4   -2.3688        +6      -7      +23     +24     +19     -20     $ form
 133    4   -2.3688        +6      -7      +23     +24     +20     -21     $ form
 134    4   -2.3688        +6      -7      +23     +24     +21     -22     $ form
c
c    ================================================================
c    ===== formation region to radius=40 cm
c    ================================================================
c
 135    4   -2.3688        +7      -8      -23     -24     +10     -11     $ form
 136    4   -2.3688        +7      -8      -23     -24     +11     -12     $ form
 137    4   -2.3688        +7      -8      -23     -24     +12     -13     $ form
 138    4   -2.3688        +7      -8      -23     -24     +13     -14     $ form
 139    4   -2.3688        +7      -8      -23     -24     +14     -15     $ form
 140    4   -2.3688        +7      -8      -23     -24     +15     -16     $ form
 141    4   -2.3688        +7      -8      -23     -24     +16     -17     $ form
 142    4   -2.3688        +7      -8      -23     -24     +17     -18     $ form
 143    4   -2.3688        +7      -8      -23     -24     +18     -19     $ form
 144    4   -2.3688        +7      -8      -23     -24     +19     -20     $ form
 145    4   -2.3688        +7      -8      -23     -24     +20     -21     $ form
 146    4   -2.3688        +7      -8      -23     -24     +21     -22     $ form
 147    4   -2.3688        +7      -8      -23     +24     +10     -11     $ form
 148    4   -2.3688        +7      -8      -23     +24     +11     -12     $ form
 149    4   -2.3688        +7      -8      -23     +24     +12     -13     $ form
 150    4   -2.3688        +7      -8      -23     +24     +13     -14     $ form
 151    4   -2.3688        +7      -8      -23     +24     +14     -15     $ form
 152    4   -2.3688        +7      -8      -23     +24     +15     -16     $ form
 153    4   -2.3688        +7      -8      -23     +24     +16     -17     $ form
 154    4   -2.3688        +7      -8      -23     +24     +17     -18     $ form
 155    4   -2.3688        +7      -8      -23     +24     +18     -19     $ form
 156    4   -2.3688        +7      -8      -23     +24     +19     -20     $ form
 157    4   -2.3688        +7      -8      -23     +24     +20     -21     $ form
 158    4   -2.3688        +7      -8      -23     +24     +21     -22     $ form
 159    4   -2.3688        +7      -8      +23     -24     +10     -11     $ form
 160    4   -2.3688        +7      -8      +23     -24     +11     -12     $ form
 161    4   -2.3688        +7      -8      +23     -24     +12     -13     $ form
 162    4   -2.3688        +7      -8      +23     -24     +13     -14     $ form
 163    4   -2.3688        +7      -8      +23     -24     +14     -15     $ form
 164    4   -2.3688        +7      -8      +23     -24     +15     -16     $ form
 165    4   -2.3688        +7      -8      +23     -24     +16     -17     $ form
 166    4   -2.3688        +7      -8      +23     -24     +17     -18     $ form
 167    4   -2.3688        +7      -8      +23     -24     +18     -19     $ form
 168    4   -2.3688        +7      -8      +23     -24     +19     -20     $ form
 169    4   -2.3688        +7      -8      +23     -24     +20     -21     $ form
 170    4   -2.3688        +7      -8      +23     -24     +21     -22     $ form
 171    4   -2.3688        +7      -8      +23     +24     +10     -11     $ form
 172    4   -2.3688        +7      -8      +23     +24     +11     -12     $ form
 173    4   -2.3688        +7      -8      +23     +24     +12     -13     $ form
 174    4   -2.3688        +7      -8      +23     +24     +13     -14     $ form
 175    4   -2.3688        +7      -8      +23     +24     +14     -15     $ form
 176    4   -2.3688        +7      -8      +23     +24     +15     -16     $ form
 177    4   -2.3688        +7      -8      +23     +24     +16     -17     $ form
 178    4   -2.3688        +7      -8      +23     +24     +17     -18     $ form
```

```
 179    4   -2.3688        +7      -8      +23     +24     +18     -19     $ form
 180    4   -2.3688        +7      -8      +23     +24     +19     -20     $ form
 181    4   -2.3688        +7      -8      +23     +24     +20     -21     $ form
 182    4   -2.3688        +7      -8      +23     +24     +21     -22     $ form
c
c    ================================================================
c    ===== formation region to radius= 60 cm
c    ================================================================
c
 183    4   -2.3688        +8      -9      -23     -24     +10     -11     $ form
 184    4   -2.3688        +8      -9      -23     -24     +11     -12     $ form
 185    4   -2.3688        +8      -9      -23     -24     +12     -13     $ form
 186    4   -2.3688        +8      -9      -23     -24     +13     -14     $ form
 187    4   -2.3688        +8      -9      -23     -24     +14     -15     $ form
 188    4   -2.3688        +8      -9      -23     -24     +15     -16     $ form
 189    4   -2.3688        +8      -9      -23     -24     +16     -17     $ form
 190    4   -2.3688        +8      -9      -23     -24     +17     -18     $ form
 191    4   -2.3688        +8      -9      -23     -24     +18     -19     $ form
 192    4   -2.3688        +8      -9      -23     -24     +19     -20     $ form
 193    4   -2.3688        +8      -9      -23     -24     +20     -21     $ form
 194    4   -2.3688        +8      -9      -23     -24     +21     -22     $ form
 195    4   -2.3688        +8      -9      -23     +24     +10     -11     $ form
 196    4   -2.3688        +8      -9      -23     +24     +11     -12     $ form
 197    4   -2.3688        +8      -9      -23     +24     +12     -13     $ form
 198    4   -2.3688        +8      -9      -23     +24     +13     -14     $ form
 199    4   -2.3688        +8      -9      -23     +24     +14     -15     $ form
 200    4   -2.3688        +8      -9      -23     +24     +15     -16     $ form
 201    4   -2.3688        +8      -9      -23     +24     +16     -17     $ form
 202    4   -2.3688        +8      -9      -23     +24     +17     -18     $ form
 203    4   -2.3688        +8      -9      -23     +24     +18     -19     $ form
 204    4   -2.3688        +8      -9      -23     +24     +19     -20     $ form
 205    4   -2.3688        +8      -9      -23     +24     +20     -21     $ form
 206    4   -2.3688        +8      -9      -23     +24     +21     -22     $ form
 207    4   -2.3688        +8      -9      +23     -24     +10     -11     $ form
 208    4   -2.3688        +8      -9      +23     -24     +11     -12     $ form
 209    4   -2.3688        +8      -9      +23     -24     +12     -13     $ form
 210    4   -2.3688        +8      -9      +23     -24     +13     -14     $ form
 211    4   -2.3688        +8      -9      +23     -24     +14     -15     $ form
 212    4   -2.3688        +8      -9      +23     -24     +15     -16     $ form
 213    4   -2.3688        +8      -9      +23     -24     +16     -17     $ form
 214    4   -2.3688        +8      -9      +23     -24     +17     -18     $ form
 215    4   -2.3688        +8      -9      +23     -24     +18     -19     $ form
 216    4   -2.3688        +8      -9      +23     -24     +19     -20     $ form
 217    4   -2.3688        +8      -9      +23     -24     +20     -21     $ form
 218    4   -2.3688        +8      -9      +23     -24     +21     -22     $ form
 219    4   -2.3688        +8      -9      +23     +24     +10     -11     $ form
 220    4   -2.3688        +8      -9      +23     +24     +11     -12     $ form
 221    4   -2.3688        +8      -9      +23     +24     +12     -13     $ form
 222    4   -2.3688        +8      -9      +23     +24     +13     -14     $ form
 223    4   -2.3688        +8      -9      +23     +24     +14     -15     $ form
 224    4   -2.3688        +8      -9      +23     +24     +15     -16     $ form
 225    4   -2.3688        +8      -9      +23     +24     +16     -17     $ form
 226    4   -2.3688        +8      -9      +23     +24     +17     -18     $ form
 227    4   -2.3688        +8      -9      +23     +24     +18     -19     $ form
 228    4   -2.3688        +8      -9      +23     +24     +19     -20     $ form
 229    4   -2.3688        +8      -9      +23     +24     +20     -21     $ form
 230    4   -2.3688        +8      -9      +23     +24     +21     -22     $ form
c
c    ================================================================
```

```
c     ===== external void
c     ============================================================
c
 231    0                 +9                                      $ exter
                       :  -10                                     $ exter
                       :  +22                                     $ exter
c
c     ============================================================
c     ===== surface cards
c     ============================================================
c     ===== general symbols
c     ============================================================
c     ============================================================
c     ===== detectors
c     ============================================================
c
   1  cy        1.27                                              $ c_nea
   2  cy        2.54                                              $ c_far
c
c     ============================================================
c     ===== tool, borehole and formation cylinders
c     ============================================================
c
   3  cy        3.81                                              $ c_too
   4  cy        8.255                                             $ c_hal
   5  c/y      -6.34        0.0         10.16                     $ c_bh
   6  c/y      -6.34        0.0         15.0                      $ c_for
   7  c/y      -6.34        0.0         25.0                      $ c_for
   8  c/y      -6.34        0.0         40.0                      $ c_for
   9  c/y      -6.34        0.0         60.0                      $ c_for
c
  10  py      -38.1                                              $ btm
  11  py       -5.0                                              $ b_sou
  12  py        5.0                                              $ t_sou
  13  py       15.24                                             $ b_nea
  14  py       22.86                                             $ t_nea
  15  py       30.0                                              $ plane
  16  py       38.1                                              $ b_far
  17  py       46.0                                              $ plane
  18  py       54.0                                              $ plane
  19  py       63.5                                              $ t_far
  20  py       70.0                                              $ plane
  21  py       82.5                                              $ plane
  22  py      101.6                                              $ top
c
c     ============================================================
c     ===== divide formation into 4 pieces
c     ============================================================
c
  23  p         1.0         0.0          1.0         0.0          $ p1
  24  p         1.0         0.0         -1.0         0.0          $ p2

c
c     ============================================================
c     ===== data cards
c     ============================================================
c
mode   n
print  110 157
```

```
drxs
nps 10000000
c
c    ===========================================================
c    ==== material #    1
c    ===========================================================
c    name    = helium-3
c    density =    0.000502 g/cc
c
   m1    2003.00c 1.00000
c
c    ===========================================================
c    ==== material #    2
c    ===========================================================
c    name    = iron
c    density =    7.8600 g/cc
c
   m2   26000.40c 1.00000
c
c    ===========================================================
c    ==== material #    3
c    ===========================================================
c    name    = borehole fluid - fw
c    density =    1.0000 g/cc
c
   m3    1001.00c 0.66667      8016.40c 0.33333
c
c    ===========================================================
c    ==== material #    4
c    ===========================================================
c    name    = formation - 20 pu limestone, fw
c    density =    2.3688 g/cc
c
   m4    1001.00c 0.15675      6012.40c 0.15298      8016.40c 0.53730
c
c    ===========================================================
c    ==== material #    5
c    ===========================================================
c    name    = formation - 1 pu limestone, fw
c    density =    2.6939 g/cc
c
   m5    1001.00c 0.00818      6012.40c 0.19755      8016.40c 0.59673
c
c
pert1:n cell=3,4,5,6,7,8,9,10,11,12,13,14 rho=-7.72
pert2:n cell=3,4,5,6,7,8,9,10,11,12,13,14 rho=-7.48
pert3:n cell=3,4,5,6,7,8,9,10,11,12,13,14 rho=-7.17
pert4:n cell=3,4,5,6,7,8,9,10,11,12,13,14 rho=-6.84
c
c
c    ===========================================================
c    ==== s(a,b) treatment
c    ===========================================================
c
mt3   lwtr.01
mt4   lwtr.01
mt5   lwtr.01
c
c    ===========================================================
```

```
c     ===== neutron source => ambe neutron source
c     ==========================================================
c
c
c         sdir     0.0    1.0    0.0  0.6  0.5
 sdef      cel=3 wgt=1 erg=d1 dir=d2 vec= 0.0 1.0 0.0
 si1                .0026126  .0408000  .0673800  .0865170
         .1110900  .1227700  .1356900  .1499600  .1647300
         .1831600  .2024200  .2237100  .2427400  .2732400
         .3019700  .3337300  .3683300  .4076200  .4504900
         .4978700  .5502300  .6081000  .6720600  .7427400
         .8208500  .9071800  1.002600  1.108000  1.224600
         1.353400  1.495700  1.653000  1.826800  2.019000
         2.231300  2.466000  2.725300  3.011900  3.328700
         3.678800  4.065700  4.493300  4.965900  5.488100
         6.065300  6.703200  7.408200  8.187300  9.048400
        10.000000 11.052000
 sp1     .000000   .005728   .003977   .002886   .003685
         .001752   .001938   .002141   .002366   .002615
         .002889   .003193   .003530   .003900   .004310
         .004764   .005265   .005819   .006431   .007107
         .007854   .008681   .009594   .010602   .011717
         .012950   .014313   .012208   .013505   .014918
         .016482   .016790   .016973   .020516   .022661
         .025052   .027678   .037100   .051803   .046116
         .046571   .051469   .063324   .068786   .051124
         .046359   .056039   .060159   .037157   .028095
         .019113
sp2    -31 0.5
c
c     ==========================================================
c     ===== tallies
c     ==========================================================
c
fq0     e  f
c
c     ==========================================================
c     =====  tally 4, neutron flux in cells 1 (near) and 2 (far)
c     ==========================================================
f4:n    1  2
fc4     neutron flux*volume in cells 1 (near) and 2 (far)
e4      0.1e-6  0.41e-6 10.6e-6 101e-6 1.5e-3 26e-3 .49 2.7 12.2 17.3
em4     1 9r
c
c     ==========================================================
c     =====  tally 24, absorption rate in cells 1 (near)
c     ==========================================================
f24:n   1
fc24    neutron absorption rate in cells 1 (near)
e24     0.1e-6  0.41e-6 10.6e-6 101e-6 1.5e-3 26e-3 .49 2.7 12.2 17.3
em24    1 9r
fm24     1.0023e-04  1  103
c
c     ==========================================================
c     =====  tally 44, absorption rate in cells 2 (far)
c     ==========================================================
f44:n   2
fc44    neutron total reaction rate in cells 1 (near) and 2 (far)
e44     0.1e-6  0.41e-6 10.6e-6 101e-6 1.5e-3 26e-3 .49 2.7 12.2 17.3
em44    1 9r
```

```
fm44    1.0023e-04  1  103
c
c    ===========================================================
c    =====  tally 64, absorption rate in cells 1 (near) and 2 (far)
c    ===========================================================
f64:n  1  2
fc64   neutron elastic scattering rate in cells 1 (near) and 2 (far)
e64    0.1e-6  0.41e-6 10.6e-6 101e-6 1.5e-3 26e-3 .49 2.7 12.2 17.3
em64   1 9r
fm64    1.0023e-04  1  2
c
c    ===========================================================
c    =====  cutoffs
c    ===========================================================
c
phys:n  14  14
cut:n   830000  0.0   -.1  -.05
thtme   0
prdmp   2j -1
ctme    3600
tmp1    0.0253e-6  230r
vol     1          230r
area    1           23r
c
c    ===========================================================
c    =====  bias parameters
c    =====       derived from xtrapt with full diffusion approximation
c    =====       (these are parameters for deriving ww from xtrapt
c    =====       adjoint fluxes).
c    ===========================================================
c    ===== adjoint fluxes          : por5xu1.
c    ===== normalization cell      :     3
c    ===== normalization group     :     2
c    ===== normalization weight    :      0.5
c    ===== minimum weight allowed  :      0.00001
c    ===== maximum weight allowed  :      1.0
c    ===== analog weight value     : 100000.0
c    =====
c    ===== number of neutron windows :     5
c    ===== number of photon  windows :     0
c    ===== number of mcnp cells      :   231
c    ===========================================================
wwp:n     5  3  5
wwe:n    4.1399-7 1.013-4 2.6058-2 2.7253 17.333
wwn1:n  5.4376e-03  5.4376e-03  5.4376e+02  5.4376e+02  1.8431e-01
        1.3183e-02  1.2343e-01  5.4376e-03  5.4376e-03  5.4376e-03
        5.4376e-03  5.4376e-03  3.9857e-01  5.4376e+02  5.4376e+02
        2.7765e+02  7.5563e-01  6.5276e-02  1.8178e-01  7.0702e-03
        5.4376e-03  5.4376e-03  5.4376e-03  2.7976e-02  2.7976e-02
        6.9505e+01  5.4376e+02  7.8168e+01  1.2746e+00  3.1653e-01
        1.8776e-01  1.5314e-02  5.4376e-03  5.4376e-03  5.4376e-03
        2.9537e-02  2.9537e-02  1.0680e+01  5.4376e+02  7.8002e+01
        6.0885e+00  1.9371e+00  4.1142e-01  8.4630e-02  2.2850e-02
        2.2850e-02  2.2851e-02  1.0777e-01  1.0777e-01  6.4436e+00
        5.4376e+02  3.0382e+01  1.0628e+00  2.2054e-01  1.0523e-01
        1.0598e-02  5.4376e-03  5.4376e-03  5.4376e-03  2.0858e-02
        2.0858e-02  2.9028e+00  5.4376e+02  3.6225e+01  9.3802e-01
        2.2052e-01  1.0528e-01  1.0603e-02  5.4376e-03  5.4376e-03
        5.4376e-03  1.9844e-02  1.9844e-02  3.4659e+00  5.4376e+02
```

```
          5.6288e+01  4.8798e-01  5.6185e-02  8.8100e-02  5.4376e-03
          5.4376e-03  5.4376e-03  5.4376e-03  1.2737e-02  1.2737e-02
          6.3683e+00  5.4376e+02  7.7442e+01  1.1057e+01  2.2675e+00
          6.0164e-01  2.0593e-01  9.7778e-02  9.7778e-02  9.7799e-02
          2.8976e-01  2.8976e-01  5.1704e+00  4.0053e+02  1.0606e+01
          1.2840e+00  2.5166e-01  6.2879e-02  1.7525e-02  8.2302e-03
          8.2302e-03  8.2311e-03  2.9484e-02  2.9484e-02  7.1153e-01
          4.1813e+02  1.1420e+01  1.4398e+00  2.5168e-01  6.2878e-02
          1.7524e-02  9.8269e-03  9.8269e-03  9.8282e-03  3.3765e-02
          3.3765e-02  7.6667e-01  2.0561e+02  4.7561e+00  4.9360e-01
          1.0839e-01  2.6856e-02  6.5165e-03  5.4376e-03  5.4376e-03
          5.4376e-03  1.0606e-02  1.0606e-02  3.1804e-01  5.4376e+02
          5.4376e+02  5.2172e+01  6.3354e+00  6.3354e+00  1.7651e+00
          8.3526e-01  8.3526e-01  8.3583e-01  8.3583e-01  2.3211e+00
          3.0391e+01  1.4502e+02  1.4502e+02  3.5676e+00  5.3502e-01
          5.3502e-01  1.4243e-01  5.1731e-02  5.1731e-02  5.1760e-02
          5.1760e-02  1.5475e-01  2.1337e+00  2.2354e+02  2.2354e+02
          5.4783e+00  8.0092e-01  8.0092e-01  2.1635e-01  8.2825e-02
          8.2825e-02  8.2873e-02  8.2873e-02  2.4264e-01  3.2576e+00
          5.8205e+01  5.8205e+01  1.4125e+00  1.9358e-01  1.9358e-01
          4.8765e-02  1.8193e-02  1.8193e-02  1.8202e-02  1.8202e-02
          5.7382e-02  8.5697e-01  5.4376e+02  5.4376e+02  1.9501e+02
          4.3795e+01  4.3795e+01  1.8594e+01  1.1175e+01  1.1175e+01
          1.1188e+01  1.1188e+01  2.2115e+01  1.2401e+02  3.1569e+02
          3.1569e+02  1.7356e+01  3.1466e+00  3.1466e+00  1.3307e+00
          1.0193e+00  1.0193e+00  1.0204e+00  1.0204e+00  2.0302e+00
          1.1171e+01  3.1575e+02  3.1575e+02  1.7358e+01  4.0853e+00
          4.0853e+00  1.7341e+00  1.0194e+00  1.0194e+00  1.0205e+00
          1.0205e+00  2.0303e+00  1.1172e+01  8.3890e+01  8.3890e+01
          4.6086e+00  1.0557e+00  1.0557e+00  4.3674e-01  2.5267e-01
          2.5267e-01  2.5294e-01  2.5294e-01  5.1594e-01  2.9604e+00
         -1.0000e+00
wwn2:n    1.7757e-02  5.4350e-04  1.5880e+00  1.5880e+00  9.6258e-02
          1.9247e-02  1.1756e-02  1.9036e-03  4.5802e-04  4.2660e-04
          4.6101e-04  2.0273e-03  9.2488e-03  7.7646e-01  1.5880e+00
          1.5880e+00  3.2581e-01  5.6523e-02  8.4317e-02  6.3782e-03
          7.9420e-04  7.6414e-04  7.9513e-04  9.9312e-03  9.9312e-03
          1.3818e+00  1.5880e+00  1.5880e+00  1.5880e+00  3.2129e-01
          2.0132e-01  1.9183e-02  3.7223e-03  3.3823e-03  3.7288e-03
          4.2937e-02  4.2937e-02  1.5880e+00  1.5880e+00  1.5880e+00
          1.5880e+00  8.6552e-01  2.2900e-01  5.6212e-02  1.6773e-02
          1.6773e-02  1.6965e-02  6.0314e-02  6.0314e-02  1.5880e+00
          1.5880e+00  1.5880e+00  7.0903e-01  1.1152e-01  4.3747e-02
          9.0062e-03  2.5991e-03  2.5991e-03  2.6214e-03  2.1023e-02
          2.1023e-02  6.2600e-01  1.5880e+00  1.5880e+00  6.0060e-01
          1.1429e-01  4.4277e-02  9.2444e-03  2.1392e-03  2.1392e-03
          2.1579e-03  1.8356e-02  1.8356e-02  5.8795e-01  1.5880e+00
          1.5880e+00  2.5971e-01  4.7687e-02  1.9363e-02  4.1038e-03
          1.0309e-03  1.0309e-03  1.0374e-03  8.5303e-03  8.5303e-03
          3.0474e-01  1.5880e+00  1.5880e+00  1.5880e+00  1.3679e+00
          4.2220e-01  1.7796e-01  9.6109e-02  9.6109e-02  9.9062e-02
          3.0572e-01  3.0572e-01  1.5880e+00  1.5880e+00  1.5880e+00
          1.0978e+00  1.7900e-01  5.2649e-02  2.0479e-02  1.1504e-02
          1.1504e-02  1.1829e-02  4.5590e-02  4.5590e-02  7.0268e-01
          1.5880e+00  1.5880e+00  1.1712e+00  1.7892e-01  5.2624e-02
          2.0222e-02  1.2029e-02  1.2029e-02  1.2354e-02  4.8261e-02
          4.8261e-02  7.4323e-01  1.5880e+00  1.5880e+00  4.6283e-01
          8.2036e-02  2.3525e-02  8.7609e-03  4.0469e-03  4.0469e-03
          4.1419e-03  1.8180e-02  1.8180e-02  3.0805e-01  1.5880e+00
```

```
        1.5880e+00  1.5880e+00  1.5880e+00  1.5880e+00  1.5880e+00
        1.4073e+00  1.4073e+00  1.4452e+00  1.4452e+00  1.5880e+00
        1.5880e+00  1.5880e+00  1.5880e+00  1.5880e+00  7.5695e-01
        7.5695e-01  2.9543e-01  1.0399e-01  1.0399e-01  1.0656e-01
        1.0656e-01  3.5910e-01  1.5880e+00  1.5880e+00  1.5880e+00
        1.5880e+00  1.1149e+00  1.1149e+00  4.3249e-01  1.6244e-01
        1.6244e-01  1.6680e-01  1.6680e-01  5.4930e-01  1.5880e+00
        1.5880e+00  1.5880e+00  1.5880e+00  2.7938e-01  2.7938e-01
        1.1265e-01  3.7097e-02  3.7097e-02  3.7806e-02  3.7806e-02
        1.3673e-01  1.5880e+00  1.5880e+00  1.5880e+00  1.5880e+00
        1.5880e+00  1.5880e+00  1.5880e+00  1.5880e+00  1.5880e+00
        1.5880e+00  1.5880e+00  1.5880e+00  1.5880e+00  1.5880e+00
        1.5880e+00  1.5880e+00  1.5880e+00  1.5880e+00  1.5880e+00
        1.5880e+00  1.5880e+00  1.5880e+00  1.5880e+00  1.5880e+00
        1.5880e+00  1.5880e+00  1.5880e+00  1.5880e+00  1.5880e+00
        1.5880e+00  1.5880e+00  1.5880e+00  1.5880e+00  1.5880e+00
        1.5880e+00  1.5880e+00  1.5880e+00  1.1394e+00  6.7161e-01
        6.7161e-01  6.9171e-01  6.9171e-01  1.5656e+00  1.5880e+00
       -1.0000e+00
wwn3:n  2.4622e-01  9.9597e-03  7.4392e-01  7.4392e-01  1.0193e-01
        2.5989e-02  9.6579e-03  2.7290e-03  7.7101e-04  7.5365e-04
        7.7837e-04  3.3590e-03  6.3425e-03  2.1031e-01  7.4392e-01
        7.4392e-01  2.8421e-01  8.3287e-02  7.1040e-02  9.6361e-03
        1.2119e-03  1.2386e-03  1.2144e-03  7.2849e-03  7.2849e-03
        4.6718e-01  7.4392e-01  7.4392e-01  7.4392e-01  6.9575e-01
        3.9413e-01  5.0412e-02  8.6695e-03  8.6385e-03  8.7032e-03
        1.0651e-01  1.0651e-01  7.4392e-01  7.4392e-01  7.4392e-01
        7.4392e-01  7.4392e-01  3.8527e-01  1.0286e-01  3.1077e-02
        3.1077e-02  3.1603e-02  1.0566e-01  1.0566e-01  7.4392e-01
        7.4392e-01  7.4392e-01  7.4392e-01  1.4784e-01  6.5230e-02
        1.4425e-02  4.3630e-03  4.3630e-03  4.4091e-03  3.9864e-02
        3.9864e-02  7.4392e-01  7.4392e-01  7.4392e-01  7.4392e-01
        1.5171e-01  6.6566e-02  1.4620e-02  3.1288e-03  3.1288e-03
        3.1621e-03  2.6527e-02  2.6527e-02  7.4392e-01  7.4392e-01
        7.4392e-01  3.6778e-01  8.6468e-02  3.4112e-02  8.8659e-03
        1.9229e-03  1.9229e-03  1.9344e-03  1.2542e-02  1.2542e-02
        4.2176e-01  7.4392e-01  7.4392e-01  7.4392e-01  7.4392e-01
        7.4392e-01  3.4520e-01  1.8035e-01  1.8035e-01  1.8771e-01
        5.6850e-01  5.6850e-01  7.4392e-01  7.4392e-01  7.4392e-01
        7.4392e-01  3.4843e-01  1.2118e-01  4.9936e-02  2.6799e-02
        2.6799e-02  2.7828e-02  1.2044e-01  1.2044e-01  7.4392e-01
        7.4392e-01  7.4392e-01  7.4392e-01  3.4999e-01  1.2104e-01
        4.8447e-02  2.5786e-02  2.5786e-02  2.6712e-02  1.2085e-01
        1.2085e-01  7.4392e-01  7.4392e-01  7.4392e-01  7.4392e-01
        1.7893e-01  6.2291e-02  2.5493e-02  1.1093e-02  1.1093e-02
        1.1453e-02  5.2194e-02  5.2194e-02  7.4392e-01  7.4392e-01
        7.4392e-01  7.4392e-01  7.4392e-01  7.4392e-01  7.4392e-01
        7.4392e-01  7.4392e-01  7.4392e-01  7.4392e-01  7.4392e-01
        7.4392e-01  7.4392e-01  7.4392e-01  7.4392e-01  7.4392e-01
        7.4392e-01  7.4392e-01  4.2981e-01  4.2981e-01  4.5174e-01
        4.5174e-01  7.4392e-01  7.4392e-01  7.4392e-01  7.4392e-01
        7.4392e-01  7.4392e-01  7.4392e-01  7.4392e-01  6.0480e-01
        6.0480e-01  6.3601e-01  6.3601e-01  7.4392e-01  7.4392e-01
        7.4392e-01  7.4392e-01  7.4392e-01  7.4392e-01  7.4392e-01
        5.2445e-01  1.7199e-01  1.7199e-01  1.7895e-01  1.7895e-01
        7.3665e-01  7.4392e-01  0.0000e+00  0.0000e+00  7.4392e-01
        7.4392e-01  7.4392e-01  7.4392e-01  7.4392e-01  7.4392e-01
        7.4392e-01  7.4392e-01  7.4392e-01  7.4392e-01  7.4392e-01
```

	7.4392e-01	7.4392e-01	7.4392e-01	7.4392e-01	7.4392e-01
	7.4392e-01	7.4392e-01	7.4392e-01	7.4392e-01	7.4392e-01
	7.4392e-01	7.4392e-01	7.4392e-01	7.4392e-01	7.4392e-01
	7.4392e-01	7.4392e-01	7.4392e-01	7.4392e-01	7.4392e-01
	7.4392e-01	7.4392e-01	7.4392e-01	7.4392e-01	7.4392e-01
	7.4392e-01	7.4392e-01	7.4392e-01	7.4392e-01	7.4392e-01
	7.4392e-01	7.4392e-01	7.4392e-01	7.4392e-01	7.4392e-01
	-1.0000e+00				
wwn4:n	5.0000e-01	1.9691e-01	5.0000e-01	5.0000e-01	1.2681e-01
	3.8540e-02	1.3447e-02	5.7967e-03	2.2949e-03	2.1411e-03
	2.3194e-03	5.6218e-03	1.0135e-02	1.1683e-01	5.0000e-01
	5.0000e-01	2.7700e-01	1.1096e-01	4.7649e-02	1.4083e-02
	3.1627e-03	3.1948e-03	3.1849e-03	9.7673e-03	9.7673e-03
	1.7272e-01	5.0000e-01	5.0000e-01	5.0000e-01	4.1226e-01
	1.5339e-01	4.4614e-02	1.3383e-02	1.2935e-02	1.3586e-02
	5.9066e-02	5.9066e-02	5.0000e-01	5.0000e-01	5.0000e-01
	5.0000e-01	5.0000e-01	2.6053e-01	1.0159e-01	3.6332e-02
	3.6332e-02	3.7116e-02	1.0615e-01	1.0615e-01	5.0000e-01
	5.0000e-01	5.0000e-01	3.9516e-01	1.1521e-01	4.4561e-02
	1.5153e-02	5.7299e-03	5.7299e-03	5.8020e-03	2.1759e-02
	2.1759e-02	2.6441e-01	5.0000e-01	5.0000e-01	3.6032e-01
	1.1377e-01	4.3817e-02	1.4560e-02	4.7054e-03	4.7054e-03
	4.7644e-03	1.8428e-02	1.8428e-02	2.2288e-01	5.0000e-01
	5.0000e-01	2.0942e-01	6.6158e-02	2.4679e-02	8.5653e-03
	3.0691e-03	3.0691e-03	3.0952e-03	1.0104e-02	1.0104e-02
	1.2849e-01	5.0000e-01	5.0000e-01	5.0000e-01	5.0000e-01
	3.5682e-01	1.7739e-01	1.0527e-01	1.0527e-01	1.0806e-01
	2.4056e-01	2.4056e-01	5.0000e-01	5.0000e-01	5.0000e-01
	5.0000e-01	1.7164e-01	6.9973e-02	3.1813e-02	1.9478e-02
	1.9478e-02	1.9909e-02	5.0191e-02	5.0191e-02	3.8875e-01
	5.0000e-01	5.0000e-01	5.0000e-01	1.6726e-01	6.7164e-02
	2.9747e-02	1.7888e-02	1.7888e-02	1.8290e-02	4.7680e-02
	4.7680e-02	3.7966e-01	5.0000e-01	5.0000e-01	3.3978e-01
	1.0372e-01	4.1477e-02	1.8368e-02	9.5938e-03	9.5938e-03
	9.7782e-03	2.5862e-02	2.5862e-02	2.1399e-01	5.0000e-01
	5.0000e-01	5.0000e-01	5.0000e-01	5.0000e-01	5.0000e-01
	5.0000e-01	5.0000e-01	5.0000e-01	5.0000e-01	5.0000e-01
	5.0000e-01	5.0000e-01	5.0000e-01	5.0000e-01	5.0000e-01
	5.0000e-01	2.7805e-01	1.3206e-01	1.3206e-01	1.3544e-01
	1.3544e-01	3.3234e-01	5.0000e-01	5.0000e-01	5.0000e-01
	5.0000e-01	5.0000e-01	5.0000e-01	3.3009e-01	1.5837e-01
	1.5837e-01	1.6231e-01	1.6231e-01	3.9974e-01	5.0000e-01
	5.0000e-01	5.0000e-01	5.0000e-01	3.8364e-01	3.8364e-01
	1.4566e-01	6.8054e-02	6.8054e-02	6.9585e-02	6.9585e-02
	1.7728e-01	5.0000e-01	5.0000e-01	5.0000e-01	5.0000e-01
	5.0000e-01	5.0000e-01	5.0000e-01	5.0000e-01	5.0000e-01
	5.0000e-01	5.0000e-01	5.0000e-01	5.0000e-01	5.0000e-01
	5.0000e-01	5.0000e-01	5.0000e-01	5.0000e-01	5.0000e-01
	5.0000e-01	5.0000e-01	5.0000e-01	5.0000e-01	5.0000e-01
	5.0000e-01	5.0000e-01	5.0000e-01	5.0000e-01	5.0000e-01
	5.0000e-01	5.0000e-01	5.0000e-01	5.0000e-01	5.0000e-01
	5.0000e-01	5.0000e-01	5.0000e-01	5.0000e-01	5.0000e-01
	5.0000e-01	5.0000e-01	5.0000e-01	5.0000e-01	5.0000e-01
	5.0000e-01	5.0000e-01	5.0000e-01	5.0000e-01	5.0000e-01
	-1.0000e+00				
wwn5:n	6.5593e-01	6.5593e-01	6.5593e-01	6.5593e-01	2.0210e-01
	7.8339e-02	2.9105e-02	1.6076e-02	1.0422e-02	9.6449e-03
	1.0641e-02	1.5536e-02	2.4605e-02	1.7456e-01	6.5593e-01
	6.5593e-01	2.3103e-01	1.0401e-01	4.6624e-02	2.3474e-02

```
      1.1987e-02  1.1445e-02  1.2216e-02  1.9814e-02  1.9814e-02
      1.3353e-01  6.5593e-01  6.5593e-01  3.6752e-01  1.5445e-01
      7.4292e-02  3.8532e-02  2.1708e-02  2.0162e-02  2.2221e-02
      4.1334e-02  4.1334e-02  2.2691e-01  6.5593e-01  6.5593e-01
      5.2755e-01  2.4782e-01  1.2794e-01  7.3619e-02  4.0502e-02
      4.0502e-02  4.1381e-02  7.5969e-02  7.5969e-02  3.5231e-01
      6.5593e-01  6.5593e-01  2.6989e-01  1.1432e-01  5.5863e-02
      3.0300e-02  1.6086e-02  1.6086e-02  1.6399e-02  3.3423e-02
      3.3423e-02  1.7551e-01  6.5593e-01  6.5593e-01  2.6242e-01
      1.1077e-01  5.3539e-02  2.8525e-02  1.4847e-02  1.4847e-02
      1.5151e-02  3.1281e-02  3.1281e-02  1.6684e-01  6.5593e-01
      6.0373e-01  1.9382e-01  7.4164e-02  3.4342e-02  1.8415e-02
      1.1271e-02  1.1271e-02  1.1454e-02  2.1263e-02  2.1263e-02
      1.1919e-01  6.5593e-01  6.5593e-01  6.5593e-01  3.8911e-01
      2.1428e-01  1.3491e-01  9.4057e-02  9.4057e-02  9.6401e-02
      1.6281e-01  1.6281e-01  6.3185e-01  6.5593e-01  6.5593e-01
      3.9118e-01  1.5444e-01  8.1239e-02  4.9417e-02  3.5943e-02
      3.5943e-02  3.6887e-02  6.5540e-02  6.5540e-02  2.7761e-01
      6.5593e-01  6.5593e-01  3.7687e-01  1.4780e-01  7.6900e-02
      4.6030e-02  3.2707e-02  3.2707e-02  3.3596e-02  6.1201e-02
      6.1201e-02  2.6451e-01  6.5593e-01  6.5593e-01  2.5556e-01
      1.0329e-01  5.3342e-02  3.2002e-02  2.1341e-02  2.1341e-02
      2.1865e-02  3.9569e-02  3.9569e-02  1.7524e-01  6.5593e-01
      6.5593e-01  6.5593e-01  6.5593e-01  6.5593e-01  6.5593e-01
      4.4861e-01  4.4861e-01  4.5836e-01  4.5836e-01  6.5593e-01
      6.5593e-01  6.5593e-01  6.5593e-01  6.5593e-01  4.4258e-01
      4.4258e-01  2.2366e-01  1.3216e-01  1.3216e-01  1.3562e-01
      1.3562e-01  2.5696e-01  6.5593e-01  6.5593e-01  6.5593e-01
      6.5593e-01  4.9646e-01  4.9646e-01  2.4892e-01  1.4945e-01
      1.4945e-01  1.5339e-01  1.5339e-01  2.9222e-01  6.5593e-01
      6.5593e-01  6.5593e-01  6.5593e-01  2.6836e-01  2.6836e-01
      1.3444e-01  7.8026e-02  7.8026e-02  7.9840e-02  7.9840e-02
      1.5446e-01  6.5593e-01  6.5593e-01  6.5593e-01  6.5593e-01
      6.5593e-01  6.5593e-01  6.5593e-01  6.5593e-01  6.5593e-01
      6.5593e-01  6.5593e-01  6.5593e-01  6.5593e-01  6.5593e-01
      6.5593e-01  6.5593e-01  6.5593e-01  6.5593e-01  6.5593e-01
      6.5593e-01  6.5593e-01  6.5593e-01  6.5593e-01  6.5593e-01
      6.5593e-01  6.5593e-01  6.5593e-01  6.5593e-01  6.5593e-01
      6.5593e-01  6.5593e-01  6.5593e-01  6.5593e-01  6.5593e-01
      6.5593e-01  6.5593e-01  6.5593e-01  6.5593e-01  5.5474e-01
      5.5474e-01  5.6948e-01  5.6948e-01  6.5593e-01  6.5593e-01
     -1.0000e+00
wwg       24 3 1.0 3.5 19.05 0
wwge:n    4.13-7 2.606-2 20
rdum       0.8
```

5. Test Problem INP14.

```
prob14 -- test general source in repeated structures.
1     1 -.5   -7 #2 #3 #4 #5 #6  imp:n=1
2     0   1 -2 -3 4 5 -6     imp:n=2  trcl=2 fill=1
3     like 2 but trcl=3
4     like 2 but trcl=4
5     like 2 but trcl=5  imp:n=1
6     like 2 but trcl=6
7     0   7 imp:n=0
8     0   8 -9 -10 11  imp:n=1 trcl=(-.9 .9 0) fill=2 u=1
```

```
9     like 8 but trcl=(.9 .9 0)
10    like 8 but trcl=(.1 -.9 0)
11    2 -18 #8 #9 #10  imp:n=1 u=1
12    2 -18   -12 imp:n=1 trcl=(-.3 .3 0) u=2
13    like 12 but trcl=(.3 .3 0)
14    like 12 but trcl=(.3 -.3 0)
15    like 12 but trcl=(-.3 -.3 0)
16    1 -.5  #12 #13 #14 #15  u=2 imp:n=1

1     px -2
2     py 2
3     px 2
4     py -2
5     pz -2
6     pz 2
7     so 15
8     px -.7
9     py  .7
10    px  .7
11    py -.7
12    cz  .1

sdef  erg=d1  cel=d2:d3:0  rad=d5  ext=d6  axs=0 0 1  pos=d7
#     si1   sp1   sb1
       1    0     0
       3    .22   .05
       4    .08   .05
       5    .25   .1
       6    .18   .1
       7    .07   .2
       8    .1    .2
       9    .05   .1
      11    .05   .2
si2   l 2 3 4 5 6
sp2     1 1 1 1 1
si3   l 8 9 10
sp3     1 1 1
si5   0 .1
sp5   -21 1
si6   -2 2
sp6    0 1
si7   l .3 .3 0   .3 -.3 0   -.3 .3 0   -.3 -.3 0
sp7   1 1 1 1
fcl:n 13j -.5  $ forced collision in lev.ne.0 geom crashes mcnp4.2
m1     6012.40c 1
m2    92235.40c 1
pert1:n   cell=1,16  rho=-1.0
pert2:n   cell=1,16  rho=-1.7
pert3:n   cell=1,16  rho=-3.5
pert4:n   cell=1,16  rho=-6.0
drxs
tr2   -6  7 1.2
tr3    7  6 1.1
tr4    8 -5 1.4
tr5*  -1 -4 1   40 130 90 50 40 90 90 90 0
tr6   -9 -2 1.3
f4:n  12 13 14 15              $ union of all 15 cell 12s, 13s, etc.
      (12 13 14 15<(u=1))      $ same as previous line, i hope
      (12 13 14 15<u=2<u=1)    $ each cylinder tallied separately
```

```
sd4   1.8849555 3r  $ 1st tally line - 15 x volume of cell 12, 13, etc.
      1.8849555 3r  $ 2nd tally line - 15 x volume of cell 12, 13, etc.
      0.1256637 3r  $ 3rd tally line - volume of cell 12, 13, etc.
fq    f e
cut:n  1e20 .1
nps   20000000
f7:n  (12<u=2<2) (12<2)    $ each cell 12 in cell 2, plus union
      (13<u=2<3) (13<3)    $ each cell 13 in cell 3, plus union
      (14<u=2<5) (14<5)    $ each cell 14 in cell 5, plus union
      (15<u=2<6) (15<6)    $ each cell 15 in cell 6, plus union
sd7   2.2619466 6.7858398   $ mass of cell 12, 3 x mass of cell 12
      2.2619466 6.7858398   $ mass of cell 13, 3 x mass of cell 13
      2.2619466 6.7858398   $ mass of cell 14, 3 x mass of cell 14
      2.2619466 6.7858398   $ mass of cell 15, 3 x mass of cell 15
fq7   f e
totnu
print -98
prdmp 2j -1
```

B. Photon Fixed-Source Problem

1. Test Problem INP04.

```
prob4 -- photons
1     1  .02  -1      $ uranium hydride ball with point source
2     2  .1 -2 1 3 4 $ uranium-lithium shell
3     0           2   $ zero-importance outside world
4     2 .1 -3 5
5     2 .1 -4 6
6     2 .1 -5
7     2 .1 -6

1     so 10
2     so 20
3     s -10 2r 2.1
4     s 10 2r 1.1
5     s -10 2r 1.9
6     s 10 2r .9

mode  p
imp:p 1 1 0 1 1 1m 1m
m1    92000 1  1000 3
m2    92000 1  3000 3
pert1:p  cell=1 rho=.0235
pert2:p  cell=1 rho=.0270
pert3:p  cell=1 rho=.0350
pert4:p  cell=1 rho=.0400
c    monoenergetic isotropic point source at (0,0,0)
sdef  erg=3   cel=1
e0    .01 .1 1 5
f6:p  1 2  6 7    $ heating tally
f5x:p   12   15   1
f4:p  1 2  6 7    $ flux tally
fq4  e f
fq6  f e
fq5  e d
fq25 e d
```

```
fz25:p -12   15  -1      -7   7   2
dd   0  100  .01
dd5  -.1
nps   25000
print -90 -98 -20 -80
prdmp 2j -1
c     dxt:p -10 2r 1 2 10 2r 1 1 .01 .005
c     dxc:p 1 1 0 .9 .9 .1 .1
pd   1 1 0 .1 3r
c     dd2  0 100 .005 .4m
de25  .01 8i .1 8i 1 2
df25 lin .8 18i .99
phys:p .05
cut:p .1 .01 .5 .2 .8
cf4  4
cf6  5
```

C. Coupled Neutron/Photon Fixed-Source Problems

1. Test Problem INP10.

```
prob10 general test problem      /x6code/gtprob
1     1  -6.4     1 -2 -31 32 -33 34
2     0           10 -4 -12 #1
3     2  -1       4 -14 -12 5
4     3  -8.94    -5 6
5     0           -6
6     4  -2.25    7 -8 -12
7     2  -1       8 -9 -12
8     2  -1       9 -12
9     4  -2.25    11 -10 -12
10    2  -1       -11 -12
11    3  -8.94    12 -13
12    0           13
13    2  -1       14 -7 -12 5

1     px 0
2     px 10
4     px 11.9
5     tx 30 0 0 20 18 18
6     tx 30 0 0 20 15 15
7     px 50
8     px 70
9     px 90
10    px -20
11    px -50
12    cx 40
13    cx 45
14    px 30
20    cx 10
21    cx 25
31    py 5
32    py -5
33    pz 5
34    pz -5

mode  n p
```

```
m1    29000.40 1  8016.40 1
m2    1001.00 2  8016.40 1
m3    29000.40 1
m4    6012.40 1
pert1:n,p cell=4,11 rho=-7.90
pert2:n,p cell=4,11 rho=-6.90
pert3:n,p cell=4,11 rho=-3.50
pert4:n,p cell=4,11 rho=-1.00
imp:n  1 1 2 2 2 4 2 1 .5 .25 1 0 4
imp:p  1 1 2 2 2 4 2 1 .5 .25 1 0 4
sdef  erg=d1 vec=1 0 0 dir=d2 pos=5 0 0 rad=d3 cel=1
sp1   -3
sb2   -31 1.2
si3   8.67
f4:n  6
f14:p 6
fq    s e
fs    -20 -21
phys:n  j 1e-6
phys:p 1 0
nps   3000000
prdmp 2j -1
print 20 -70 50 -72 100 -30 -98
```

2. Test Problem INP11.

```
prob11 -- intertwined super pretzels with s(a,b), mode n p
1     1 -7.8   -1:-2:-3   $ pretzel of tori
2     2 -2.66  -4:-5:-6:-7:-8:-9:-10:-11   $ cage of ellipsoids
3     3 -9     -12 -13:-14:-15:-16:-17:-18:-19:-20:-21   $ toys
4     4 -.5    1 2 3 4 5 6 7 8 9 10 11(12:13)   $ space between
                14 15 16 17 18 19 20 21 -22
5     0        22        $ zero-importance outside world
6     0        -23 -24 -25 26   $ cookie-cutter cell

1     tx 0 0 0 10 2 2
2     ty 0 0 0 12 2 2.5
3     tz 0 0 0 10 3 4
4     sq .028 1 1 0 0 0 -1 0 15 5
5     sq 1 .00448 1 0 0 0 -1 -5 0 5
6     sq 1 1 .028 0 0 0 -1 -5 -15 0
7     sq 1 .00448 1 0 0 0 -1 -5 0 -5
8     sq .028 1 1 0 0 0 -1 0 15 -5
9     sq 1 .00448 1 0 0 0 -1 5 0 -5
10    sq 1 1 .028 0 0 0 -1 5 -15 0
11    sq 1 .00448 1 0 0 0 -1 5 0 5
12    sq .1 0 .05 0 1 0 -4 0 -11 17
13    sq .1 0 .07 0 -.3 0 -10 0 -1 16
14    sq .05 .2 1 0 0 0 -16 0 -6 -20
15    sq 1 .1 1 0 0 0 -4 0 14 -14
16    sq 1 1 .1 0 0 0 -4 0 14 -14
17    s 0 4.5 22.5 2
18    s 0 6.5 22.5 2
19    s 0 5.5 18 4
20    s 0 4.5 14 1
21    s 0 6.5 14 1
22    so 30
23    pz 9
```

```
24     c/y 1 .5 10
25     py -18.5
26     py -21.5

m1     92235.40c 1
m2     14000.40c 1 8016.40c 2
m3     29000.40c 1
m4     1001.00c 2 8016.40c 1
mt4    lwtr.01t
pert1:n,p  cell=1  rho=-8.75   $ 5% increase in tally 4
pert2:n,p  cell=1  rho=-9.50   $ 10% increase in tally 4
pert3:n,p  cell=1  rho=-10.90  $ 20% increase in tally 4
pert4:n,p  cell=1  rho=-12.00  $ 30% increase in tally 4
imp:n 1 1 1 1 0 0
mode  n p
c    monodirectional source on plane with cookie cutter
sdef  pos 0 -20 0  dir 1  vec .05 1 .1  rad d1  axs .05 1 .1
      ccc 6  erg d2
si1   0 12
si2   1e-8 .001
sp2   0 1
cut:n  1000 0 .2 .1
fq    f e
f4:n    1 2 3
sd4    (1) (1) (1)
fc4  volumes=1. so tally is volume-integrated flux
e4    1e-7 .001 20
f11:p   1 2 3 t
tf11   4
tmp1  4e-8 3r 0 0
nps   5000000
print  -98 -85
prdmp 2j -1
```

D. Criticality Problems

1. Test Problem INP09.

```
prob9 -- kcode in complicated cells and sdef
1     1 -14.1   -1 2 3(-4:-16)5 -6(12:13:-14)(10:-9:-11:-7:6)15
2     2 -7.58   -10 9 11 7 -6 -1:2 -12 14 -6 -13 3
3     3 -.01    -17(1:-2:-5:6:-3:-15:16 4)
4     0 17

1     pz 10
2     pz -10
3     py -10
4     py 10
5     px -10
6     px 10
7     px -1
9     py -2
10    py 0
11    pz 5
12    pz -8
13    py -3
14    px 2
```

```
15    3 kx  1 .3 1 $ MCNP4.2 cone rotation bug (X-6:HGH-92-337)
16    2 kz 13 1 -1 $ MCNP4.2 cone rotation bug (X-6:HGH-92-337)
17    so 20

imp:n 1 1 1 0
tr3   0 0 0  0 -1 0  1 0 0  0 0 1
tr2   0 0 0  1 0 0  0 0 -1  0 1 0
kcode 150000 1 10 210
sdef  cel=1 x=d3 y=d2 z=d1
si1   -10 10
sp1    0  1
si3   -10 10
sp3    0  3
si2   -10 10
sp2    0  2
m1    92235.40c 1  $ test of getting 92235.51c instead
m2    29000.40c -1  $ test getting 29000.51c instead
m3    8016.40c 1  7014.40c 1
pert1:n  cell=3  rho=-0.49
pert2:n  cell=3  rho=-0.90
pert3:n  cell=3  rho=-2.00
pert4:n  cell=3  rho=-3.0
print -98
prdmp 2j -1
f7:n   1 2 3
vol  1 j 1
fq0   e f
f4:n   1 2 3
f14:n  1
fm14  -1 1 -6 -7
sd14   1
fc14   keff estimator for cell 1
e0                .162524  .266043  .358425  .445672  .530293  .613680
        .696783  .780264  .864702  .950540 1.038286 1.128326 1.221111
       1.317206 1.417070 1.521302 1.630646 1.745929 1.868073 1.998282
       2.138046 2.289259 2.454356 2.636707 2.840830 3.073518 3.344965
       3.672134 4.086420 4.656234 5.588725 9.000000
c      ssw  cel 1
```

2. Test Problem INP18.

```
prob18 -- kcode in a hexagonal prism lattice
c     three half control rods and five whole control rods.
30    0 -905 -19 29 1  fill=1
31    0 -906 -19 29 1  fill=1 (16.7113 0 0)
37    0 -907 -19 29 1  fill=1 (-16.7113 0 0)
34    0 -913 -19 29    fill=1 (0 11.9185 0)
32    0 -914 -19 29    fill=1 (10.3217 5.9592 0)
33    0 -915 -19 29    fill=1 (8.3557 14.4724 0)
35    0 -916 -19 29    fill=1 (-8.3557 14.4724 0)
36    0 -917 -19 29    fill=1 (-10.3217 5.9592 0)
c     universe 1:  structure of control rod.
38    11  -2.02      -880  u=1   $ control rod core
39     6  -8.4   880 -881  u=1   $ control rod cladding
40    12  -1.00  881 -882  u=1   $ control rod gap
41     6  -8.4   882       u=1   $ control rod sheath
c     the space between the control rods, filled with lattice.
140   0  -17 1 29 -19 905 906 907 913 914 915 916 917  fill=2
```

```
c     universe 2:  lattice of fuel rods with water in between.
42    12 -1.00   -301 302 -303 304 -305 306   u=2   lat=2   fill=
      -37:27 -1:33 0:0 &
      2 4r 3 9r 2 4r 3 11r 2 4r 3 11r 2 4r 3 9r 2
      2 4r 3 9r 2 3r 3 12r 2 3r 3 12r 2 3r 3 9r 2 1r
      2 3r 3 10r 2 2r 3 13r 2 2r 3 13r 2 2r 3 10r 2 1r
      2 3r 3 57r 2 2r &
      2 2r 3 58r 2 2r
      2 2r 3 16r 2 2r 3 17r 2 2r 3 16r 2 3r
      2 2r 3 15r 2 3r 3 16r 2 3r 3 15r 2 4r
      2 1r 3 15r 2 4r 3 15r 2 4r 3 15r 2 4r
      2 1r 3 15r 2 3r 3 16r 2 3r 3 15r 2 5r
      2 1r 3 15r 2 2r 3 17r 2 2r 3 15r 2 6r
      2 1r 3 54r 2 7r &
c       can code remember & thru comment?
 2 3 55r 2 7r
      2 3 25r 2 2r 3 25r 2 8r
      2 3 24r 2 3r 3 24r 2 9r
      2 3 23r 2 4r 3 23r 2 10r
      2 3 15r 2 2r 3 4r 2 3r 3 4r 2 2r 3 15r 2 11r
      2 3 14r 2 3r 3 4r 2 2r 3 4r 2 3r 3 14r 2 12r
      2 3 13r 2 4r 3 11r 2 4r 3 13r 2 13r
      2 3 13r 2 3r 3 12r 2 3r 3 13r 2 14r
      2 3 13r 2 2r 3 13r 2 2r 3 13r 2 15r
      2 3 46r 2 16r
      2 3 45r 2 17r
      2 3 44r 2 18r
      2 1r 3 41r 2 20r
      2 1r 3 40r 2 21r
      2 1r 3 39r 2 22r
      2 2r 3 36r 2 24r
      2 2r 3 35r 2 25r
      2 3r 3 32r 2 27r
      2 4r 3 29r 2 29r
      2 5r 3 26r 2 31r
      2 6r 3 23r 2 33r
      2 8r 3 18r 2 36r
      2 11r 3 11r 2 40r
      2 64r
c     universe 3:  structure of fuel rod lattice elements.
154   2 -13.75        -58     u=3   $ fuel element
149  12  -1.00     58 -268    u=3   $ gap
144   7 -19.66    268 -478    u=3   $ liner
159   6  -8.4     478 -698    u=3   $ cladding
141  12  -1.00    698         u=3   $ water between the fuel rods
162    0 17:-29:19:-1    $ outside world

    *1    py   0       $ x-z plane, reflective
17    cz  29.135
19    pz  31.75    $ top of reactor
29    pz -31.75    $ bottom of reactor
58    c/z     3.4414     .8515     .3240
268   c/z     3.4414     .8515     .3345
478   c/z     3.4414     .8515     .3475
698   c/z     3.4414     .8515     .4318
880   cz   1.7251
881   cz   1.8051
882   cz   1.9051
905   cz   2.1055
```

```
906   c/z  16.7113 0 2.1055
907   c/z  -16.7113 0 2.1055
913   c/z  0 11.9185 2.1055
914   c/z  10.3217 5.9592 2.1055
915   c/z  8.3557 14.4724 2.1055
916   c/z  -8.3557 14.4724 2.1055
917   c/z  -10.3217 5.9592 2.1055
301   px 3.9330
302   px 2.9498
303   p   1 1.7320508076 0  5.8994
304   p   1 1.7320508076 0  3.9330
305   p  -1 1.7320508076 0  -.9834
306   p  -1 1.7320508076 0 -2.9498

imp:n    1   18r   0
m2      92235.40c  -.70573    92238.40c  -.23821     7014.40c  -.05605
m6      41093.40c  -.99000    40000.40c  -.01000
m7      74000.40c  -.74000
m11      5010.03d  -.6870      5011.40c  -.0840      6012.40c  -.2290
m12      1001.00c 1   1002.55c 1   8016.40c 1
mt12     hwtr.01 lwtr.01
pert1:n  cell=42,141,40,149  rho=-1.50
pert2:n  cell=42,141,40,149  rho=-2.30
pert3:n  cell=42,141,40,149  rho=-4.00
pert4:n  cell=42,141,40,149  rho=-6.0
kcode    40000   1  10 210
ksrc   3 .2 .2 .2 3 .2 -3 .2 .2 .2 3 .2 4 3 .2 -4 3 .2 4 3 .1 -4 3 .2
e     .01 .1 1. 10.
fq    f e
fc4   fuel rod flux in 5 y locations averaged over 5 x elements
f4:n  (154<(42[-10:-6 -1 0]))   $ average 5 x elements at j=-1
      (154<(42[-10:-6  3 0])) &  $ average 5 x elements at j=3
(154<(42[-10:-6 10 0]))   $ average 5 x elements at j=10 &
      (154<(42[-10:-6 21 0]))   $ average 5 x elements at j=21
      (154<(42[-10:-6 29 0]))   $ average 5 x elements at j=29
sd4   104.7089062 4r            $ 5 times the volume of cell 154
f14:n  154
fm14   -1 2 -6 -7
sd14   1
fc14   keff estimator for cell 154
print -98
prdmp 2j -1
c     ptrac buffer=20 file=asc write=all event=bnk
```

APPENDIX B

ADDITIONAL PERTURBATION EXAMPLES

I. OVERVIEW

The perturbations presented in Section IV of this report are deliberately simplistic to facilitate the verification effort. The examples given in this appendix represent more complex perturbations and demonstrate the flexibility of the PERT card. These examples were derived from test problem INP04 (see Appendix A) and represent three categories of perturbations: voiding and unvoiding, composition and geometric perturbations, and sensitivity estimates.

A. Voiding and Unvoiding

Voiding a cell is simply an extension of a density change, using the keywords CELL and RHO on the PERT card, with the density set to zero. Unvoiding a cell cannot be directly performed using this technique; however, a simple solution is to include the material in the unperturbed problem. In this approach, the cell of interest is modeled with the material and the PERT card simply voids the cell. The sign of the perturbation results should be reversed in the case of unvoiding. The following MCNP example includes a sphere of UH_3 surrounded by a void spherical shell and a layer of ULi_3.

```
Appendix B sample problem 1
1     1  .02  -1     imp:p=1  $ UH3 inner sphere
2     0        1 -2  imp:p=1  $ Void spherical shell
3     2  .1    2 -3  imp:p=1  $ ULi3 outer shell
4     0        3     imp:p=0  $ Outside world

1     so 10
2     so 10.5
3     so 20

mode  p
m1    92000 1  1000 3          $ Uranium Hydride
m2    92000 1  3000 3          $ Uranium Lithium
sdef  erg=6                    $ 6 MeV source at center
f1:p  3                        $ Current on outer surface
nps   25000
```

To unvoid cell 2 with ULi_3, simply fill cell 2 with ULi_3, add a PERT card that voids cell 2, and reverse the sign of the perturbation estimate for Tally 1. These modifications are included in the following input file.

```
Appendix B sample problem 1
1     1  .02  -1      imp:p=1  $ UH3 inner sphere
2     2  .1    1 -2   imp:p=1  $ ULi3 inner shell
3     2  .1    2 -3   imp:p=1  $ ULi3 outer shell
4     0        3      imp:p=0  $ Outside world

1     so 10
2     so 10.5
3     so 20

mode  p
m1    92000 1  1000 3          $ Uranium Hydride
m2    92000 1  3000 3          $ Uranium Lithium
pert1:p  cell=2 rho=0.
sdef  erg=6                    $ 6 MeV source at center
f1:p  3                        $ Current on outer surface
nps   25000
```

Clearly if one wants to unvoid a region with several different materials, then separate runs must be performed.

B. Composition and Geometric Perturbations

A composition perturbation can range from a slight variation in atom or weight fractions to a change in material. Variations in atom or weight fractions are straightforward and require only an additional material card, reflecting the fractional changes, and the use of the CELL and MAT keywords on the PERT card (the RHO keyword may also be used to alter the density). Problem INP02 of Section IV is an example of such a perturbation. Changes in material, on the other hand, are somewhat more complicated. In this case, the unperturbed problem must be modified such that cells of interest contain a mixture of both materials (the original material plus the perturbation material). Furthermore, two PERT cards are required to estimate the change back to the original material *and* to the perturbation material. Finally, these two perturbation results must be properly combined to obtain the overall estimate for the material perturbation. Consider the previous example, except that this time cell 2 is filled with UH_3.

```
Appendix B sample problem 2
1     1  .02  -1     imp:p=1  $ UH3 inner sphere
2     1  .02   1 -2  imp:p=1  $ UH3 inner shell
3     2  .1    2 -3  imp:p=1  $ ULi3 outer shell
4     0        3     imp:p=0  $ Outside world

1     so 10
2     so 10.5
3     so 20

mode  p
m1    92000 1  1000 3          $ Uranium Hydride
m2    92000 1  3000 3          $ Uranium Lithium
sdef  erg=6                    $ 6 MeV source at center
f1:p  3                        $ Current on outer surface
nps   25000
```

The effect of changing cell 2 from UH_3 to ULi_3 can be estimated with the following steps. First, fill cell 2 with a mixture of UH_3 and ULi_3. The new material card needed for this cell can be obtained by simply adding the atom fractions of the separate materials. This same approach can be used for weight fractions as well. As long as a significant amount of each material is in the mixture, the way they are combined is not important. Next, add two PERT cards — one that perturbs cell 2 back to UH_3 and one that perturbs cell 2 to ULi_3. This leads to the following input file.

```
Appendix B sample problem 2
1     1  .02  -1     imp:p=1  $ UH3 inner sphere
2     3  .06   1 -2  imp:p=1  $ Mixture of UH3 and ULi3
3     2  .1    2 -3  imp:p=1  $ ULi3 outer shell
4     0        3     imp:p=0  $ Outside world

1     so 10
2     so 10.5
3     so 20

mode  p
m1    92000 1  1000 3          $ Uranium Hydride
m2    92000 1  3000 3          $ Uranium Lithium
m3    92000 2  1000 3 3000 3   $ Half UH3 and ULi3
pert1:p  cell=2 mat=1 rho=.02
pert2:p  cell=2 mat=2 rho=.1
sdef  erg=6                    $ 6 MeV source at center
f1:p  3                        $ Current on outer surface
nps   25000
```

Note that the density of cell 2 is consistent with the mixture of UH_3 and ULi_3. The exact value of this density is not important, as long as it is between the densities of the two materials. It should also be noted that the unperturbed results for Tally 1 will change from that of the previous input

file, since they are now consistent with the mixture of materials in cell 2. Finally, properly combining the perturbation results is important. To estimate the change of going *from* UH_3 *to* ULi_3, take PERT2 minus PERT1. To estimate the change of going *from* ULi_3 *to* UH_3, take PERT1 minus PERT2.

Geometric perturbations are included in this section since they can be modeled, in most cases, as material perturbations. Such perturbations are achieved in MCNP by overspecifying the geometry in the region of interest. For example, the previous problem can be viewed as a geometric perturbation in that it gives the estimated effect of the ULi_3 region collapsing into the UH_3 region. In a similar manner, one could consider the effect of withdrawing a control rod in a nuclear reactor. Simply model the region of motion as a separate cell and perturb the material in that cell from control rod material to moderator material, for example.

C. Sensitivity Estimates

Sensitivity calculations are also possible with the PERT card. While such calculations typically include only the first order coefficient of the Taylor Series expansion, in MCNP both the first and second order coefficients can be separately obtained. The only trick to performing sensitivity analyses is creating material cards that produce 100% increases in one or more constituents of a material. The general approach is to add a new material card for each constituent of interest. In these material cards, simply double the atom or weight fraction associated with the constituent of interest. To avoid fractional changes in the other constituents, the cell density should be multiplied by the ratio of the perturbed fractional sum to the unperturbed fractional sum. While this may sound difficult, in practice it is rather simple. For example, to double (i.e., 100% increase) the hydrogen in UH_3, simply create a material with one atom of uranium for every six atoms of hydrogen. To avoid perturbing the fraction of uranium, the density is increased by the ratio of (1+6)/(1+3)=7/4. Similarly, to double the uranium in UH_3, mix two atoms of uranium with three atoms of hydrogen and multiply the density by (2+3)/(1+3)=5/4. In addition to obtaining sensitivities to 100% increases in particular constituents, one can apply these increases to specific reactions (i.e., elastic, inelastic, absorption, etc. cross sections) over a specified energy range with use of the RXN and ERG keywords. By default, increases are applied to the total cross section and over all energies. The following input file gives examples of some of these combinations.

```
Appendix B sample problem 3
1     1  .02  -1      imp:n=1  $ UH3 inner sphere
2     2  .1    1 -2   imp:n=1  $ ULi3 inner shell
3     2  .1    2 -3   imp:n=1  $ ULi3 outer shell
4     0        3      imp:n=0  $ Outside world

1     so 10
2     so 10.5
3     so 20

mode  n
m1    92235 1  1001 3          $ Uranium Hydride
m2    92235 1  3006 3          $ Uranium Lithium
m3    92235 1  1001 6          $ 100% more H in UH3
m4    92235 2  1001 3          $ 100% more U in UH3
m5    92235 1  3006 6          $ 100% more Li in ULi3
m6    92235 2  3006 3          $ 100% more U in ULi3
pert1:n  cell=1 mat=3 rho=.035 rxn=2 method=2
pert2:n  cell=1 mat=4 rho=.025 rxn=102 method=2
pert3:n  cell=2 mat=5 rho=.175 rxn=-2 erg=1,2 method=2
pert4:n  cell=2 mat=6 rho=.125 rxn=16 method=2
sdef  erg=6                    $ 6 MeV source at center
f1:n  3                        $ Current on outer surface
nps   50000
```

Note that this input file differs from the previous examples in that it has been switched to neutron mode to demonstrate the numerous reactions available for sensitivity analysis. Also note that materials 3-6 are applied only to the PERT cards and they provide 100% increases in each constituent of the two original materials. The first PERT card gives the sensitivity of Tally1 to a 100% increase in the hydrogen elastic cross section of cell 1. As one might expect, this perturbation generates a large positive sensitivity to Tally 1 (i.e., increasing the hydrogen scatter will increase the moderation which produces more fissions). The second PERT card produces the sensitivity of Tally 1 to a 100% increase in the uranium (n,γ) cross section of cell 1. This sensitivity coefficient is significant and negative. The third PERT card gives the sensitivity of Tally 1 to a 100% increase in the lithium absorption cross section (from 1-2 MeV) of cell 2. Being a small region and a small energy range, this sensitivity has a small negative value. The last PERT card produces the sensitivity of Tally 1 to a 100% increase in the uranium (n,2n) cross section of cell 2. This sensitivity is also small, but positive (i.e., increasing this cross section results in more neutrons exiting the outer surface). A description of the various RXN values can be found in Ref. 1. Note that these four PERT cards use the METHOD keyword to obtain only the first order coefficient. An additional four PERT cards could be added with METHOD=3 to separately obtain the second order coefficients.

APPENDIX C

STATISTICAL EQUATIONS

I. ACTUAL RESULTS

The "actual" perturbation results presented in Section IV were calculated by performing four separate MCNP runs - one for each of the four perturbations. The percent change in a tally was calculated using the following standard equation

$$A = \frac{(t_p - t_u)}{t_u} \times 100$$

were t_u is the value of the unperturbed tally and t_p is the value of the perturbed tally. The unperturbed tally was obtained from the "predicted" run discussed below. If r_u and r_p are the relative errors for t_u and t_p, standard error propagation (assuming the separate MCNP runs are independent) results in the following equation for the relative error of A

$$r_A = \frac{\sigma_A}{A} = \sqrt{\frac{(t_p r_p)^2 + (t_u r_u)^2}{(t_p - t_u)^2} + r_u^2}$$

This equation was used to calculate the relative error associated with the actual perturbation results. Clearly, as the magnitude of the perturbation vanishes (i.e., t_p-t_u -> 0), the relative error of the change becomes unbounded. For most applications, this trend becomes evident when the magnitude of the perturbation is less than 1% (see the results for problems INP10 and INP12 in Section IV), rendering this perturbation approach useless.

II. PREDICTED RESULTS

The "predicted" perturbation results presented in Section IV were calculated in one MCNP run with four PERT cards. In addition to generating the unperturbed tally with this run, each PERT card produced the predicted *differential change* in the tally of interest for that perturbation. Thus, the percent change in the tally of interest simply becomes

$$P = \frac{\Delta t}{t_u} \times 100$$

where t_u is the value of the unperturbed tally and Δt is the predicted differential change in the unperturbed tally. If r_u and $r_{\Delta t}$ are the relative errors for t_u and Δt, standard error propagation gives the following equation for the relative error of P

$$r_P = \frac{\sigma_P}{P} = \sqrt{r_{\Delta t}^2 + r_u^2}$$

This equation was used to calculate the relative error associated with the predicted perturbation results. A key advantage of the differential operator technique is evident here; namely the relative error associated with the estimator is always bounded.

APPENDIX D

NON-STANDARD RESPONSES

I. LINEAR RESPONSE FUNCTIONS

The derivation of the first and second order coefficient estimators is presented in Section II with the assumption that the path segment response estimator, $t_{j'}$, is independent of the perturbed cross section, $x_b(h)$. This is the case for standard flux (i.e., track-length estimator) tallies. However, there are other Monte Carlo estimators for which this is not the case, for example k_{eff}, reaction rate, heating, etc. While it is difficult to generalize the implications of such nonstandard responses, the following sections describe the necessary modifications for linear response functions.

A. First Order

The first order differential operator, $\gamma_{1j'}$, must be modified to include the term

$$R_{1j'} = \sum_{b \in B} \sum_{h \in H} x_b(h) \left(\frac{1}{t_{j'}}\right) \left(\frac{\partial t_{j'}}{\partial x_b(h)}\right)$$

where now $t_{j'}$ is a function of $x_b(h)$. For most applications, the tally response is a linear function of $x_b(h)$, or

$$t_{ij'} = \lambda_k \cdot x_b(h)$$

(e.g., a track length estimator of a reaction rate) in which case

$$R_{1j'} = \sum_{b \in B} \sum_{h \in H} x_b(h) \left(\frac{1}{\lambda_k \cdot x_b(h)}\right) \lambda_k = 1$$

For example, if $t_{j'}$ is the tritium breeding in a material that contains only ^{6}Li and $x_b(h)$ is the ^{6}Li(n,α)t cross section, then $R_{1j'}$ =1. However, if $t_{j'}$ is the tritium breeding in a material with ^{6}Li and ^{7}Li and $x_b(h)$ is again the ^{6}Li(n,α)t cross section, then $R_{1j'}$ becomes

$$R_{1j'} = {}^{6}Li(n,\alpha)\,t\left(\frac{1}{\lambda_k \cdot \left[{}^{6}Li(n,\alpha)\,t + {}^{7}Li(n,n')\,t\right]}\right)\lambda_k$$

$$= \frac{{}^{6}Li(n,\alpha)\,t}{{}^{6}Li(n,\alpha)\,t + {}^{7}Li(n,n')\,t}$$

Adding $R_{1j'}$ to $\gamma_{1j'}$ modifies the first order coefficient estimator such that

$$\langle u_1 \rangle = \frac{1}{N}\sum_i \left[\sum_j \left(\sum_{k=0}^{m} \beta_{j'k} + R_{1j'}\right) t_{j'}\right]$$

where $\beta_{j'k}$ is defined in Section II.A and $R_{1j'} = x_b(h)/x_r$ when $t_{j'} = \lambda_k * x_r$ is some linear function of $x_b(h)$.

B. Second Order

For second order perturbations, the complexity of $\gamma_{2j'}$ appears significant for responses that are a function of $x_b(h)$; however, it is easy to show that if $t_{j'}$ is a linear function of $x_b(h)$, then

$$\frac{\partial^2 t_{j'}}{\partial x_b^2(h)} = 0$$

and the second order coefficient estimator becomes

$$\langle u_2 \rangle = \frac{1}{2N}\sum_i \left[\sum_j \left(\left(\sum_{k=0}^{m} \beta_{j'k} + R_{1j'}\right)^2 + \sum_{k=0}^{m} (\alpha_{j'k} - \beta_{j'k}^2) - R_{1j'}^2\right) t_{j'}\right]$$

where $\beta_{j'k}$ is given in Section II.A, $\alpha_{j'k}$ is given in Section II.B, and $R_{1j'}$ is described above.

Los Alamos
NATIONAL LABORATORY
Los Alamos, New Mexico 87545